2021, **22** (2), 87–107. DOI: 10.26089/NumMet.v22r207

DOI: 10.26089/NumMet.v22r207

Explicit higher-order schemes for molecular dynamics problems

E. V. Vorozhtsov
Khristianovich Institute of Theoretical and Applied Mechanics, Siberian Branch of Russian Academy of Sciences, Novosibirsk, Russia
ORCID: http://orcid.org/0000-0003-2753-8399, e-mail: vevg46@mail.ru

S. P. Kiselev
Khristianovich Institute of Theoretical and Applied Mechanics, Siberian Branch of Russian Academy of Sciences, Novosibirsk, Russia
ORCID: http://orcid.org/0000-0001-9659-7005, e-mail: kiselev@itam.nsc.ru

Abstract: The Runge–Kutta–Nyström (RKN) explicit symplectic difference schemes are considered with a number of stages from 1 to 5 for the numerical solution of molecular dynamics problems described by systems with separable Hamiltonians. For the numbers of stages 2 and 3, the parameters of the RKN schemes are obtained using the Gröbner basis technique. For the number of stages 4 and 5, new schemes were found using the Nelder–Mead numerical optimization method. In particular, four new schemes are obtained for the number of stages 4. For the number of stages 5, three new schemes are obtained in addition to the four schemes, which are well-known in the literature. For each specific number of stages, a scheme is found being the best in terms of the minimum of the leading term of the approximation error. Verification of the schemes is carried out on a problem that has an exact solution. It is shown that the symplectic five-stage RKN scheme provides a more accurate conservation of the total energy balance of the particle system than schemes of lower orders of accuracy. The stability studies of the schemes were performed using the *Mathematica* software package.

Keywords: molecular dynamics, Hamilton equations, symplectic difference schemes, stability.

Acknowledgements: The work was supported in part by the Russian Foundation for Basic Research (grant No. 19-01-00292-a) and the Program of Basic Research of State Academies of Sciences for 2013-2020 (projects AAAA-A17-117030610134-9, AAAA-A17-117030610124-0).

For citation: E. V. Vorozhtsov and S. P. Kiselev, "Explicit higher-order schemes for molecular dynamics problems," Numerical Methods and Programming. **22** (2), 87–107 (2021). doi: 10.26089/NumMet.v22r207.

1. Introduction. One of the most relevant directions of contemporary research in solid state mechanics is the study of material behavior under shock-wave load using molecular dynamics (MD) methods. This area of research emerged in mid-20th century, with the advent of new pulse technologies, which required high concentrations of energy. The essence of the MD method is to solve the equations describing motion of atoms interacting through a potential that depends on the coordinates of the atoms. This method does not require formulating state equations. It is well known that obtaining these equations is one of the most challenging problems in continuum mechanics [1].

Another advantage of the molecular dynamics method as compared to the classical continuum mechanics is that the MD method naturally takes into account the effect of the solid bodies' crystal structure on their deformation and fracture processes under dynamic loads.

As shown in [2], within a limit where the number of particles in a volume tends to ∞, the MD equations are transformed to the well-known continuum mechanics equations, which were studied and solved in [1] using the *Mathematica* software package.

2021, **22** (2), 87–107. DOI: 10.26089/NumMet.v22r207

The molecular dynamics equations are formulated as ordinary differential Hamilton equations for atoms in a solid body. MD equations have an exact analytical solution in a very limited number of cases [3]. Therefore, as a general rule, these equations are solved numerically, using difference schemes in which the differential operator is replaced by a difference operator.

When solving the Hamilton equations, it is natural to use difference schemes that preserve the symplectic properties of these equations. Violating this condition results in a failure to preserve the Poincaré invariants and introduction of non-physical instability in numerical calculations [4]. It follows that the difference operator in the numerical scheme should possess the canonical transformation properties. The symplectic difference schemes are constructed using operator method [5-8] and the RKN method [7, 9–11].

Explicit difference schemes are known to impose a limitation on the integration step [2, 12]. On the other hand, the advantage of explicit schemes is the simplicity of their software implementation. In addition, the increases in performance of desktop computers enables solving many important application tasks within a reasonable time using explicit schemes. Therefore, explicit difference schemes are preferred in this paper.

Numerical methods for solving MD problems are developing rapidly. Despite the apparent simplicity of the MD method, the issues of accuracy, stability and dispersion of difference schemes for MD problems have not been fully investigated so far.

According to the theory of Hamilton's equations, the law of conservation of total energy of the particles system must be fulfilled [3]. It is natural to demand that the difference scheme must also meet the requirement for conservation of total energy. However, as the computational practice shows, imbalance of the total energy in the system turns out to be more significant for explicit symplectic difference RKN schemes of low orders of accuracy (second- and third-order). At the same time, it is shown in [12] that a three-stage RKN scheme of fourth-order accuracy provides less error in energy imbalance than the second- and third-order accuracy schemes. Hence, it is reasonable to develop explicit symplectic RKN schemes of higher orders of accuracy. As was shown in [12], the derivation of symplectic three-stage RKN schemes involves a large amount of symbolic computation. These computations were performed in [12] using the *Maple 12* software package.

For all RKN schemes, the systems of polynomial equations that the weight parameters should satisfy to provide the highest accuracy for a given number of stages, are presented below. The solutions of polynomial systems are found for numbers in stages 2 and 3 using Gröbner bases. We must note that the available publications on RKN schemes provide incomplete information on the stability regions. In particular, we were unable to find this information in the case of two-, four-, and five-stage RKN schemes. We fill the gap in this article. The schemes have been verified by comparing numerical solutions with the exact solution of the test problem. It is shown that the symplectic five-step RKN scheme provides more accurate conservation of the total energy balance of the particle system than schemes with lower-order accuracy described in [2, 12].

2. Basic Equations. In the molecular dynamics method the calculation of N particle motion is carried out by solving Hamilton's equations

$$\begin{cases} \dfrac{dx_{i\alpha}}{dt} = \dfrac{\partial H}{\partial p_{i\alpha}}, \\ \dfrac{dp_{i\alpha}}{dt} = -\dfrac{\partial H}{\partial x_{i\alpha}}, \\ H(x_{i\alpha}, p_{i\alpha}) = K(p_{i\alpha}) + V(x_{i\alpha}), \\ K(p_{i\alpha}) = \sum\limits_{i=1}^{N} \sum\limits_{\alpha=1}^{3} \dfrac{p_{i\alpha}^2}{2m_i}, \end{cases} \tag{1}$$

where i is the particle number, α is the coordinate number $x_{i\alpha}$ and momentum number $p_{i\alpha}$, m_i is the particle mass, $K(p_{i\alpha})$ is the kinetic energy, $V(x_{i\alpha})$ is the potential energy of the interaction of particles, $H(x_{i\alpha}, p_{i\alpha})$ is the Hamiltonian of the particle system. The solution of the system of equations (1) given initial conditions $x_{i\alpha}(t=0) = x_{i\alpha}^0$, $p_{i\alpha}(t=0) = p_{i\alpha}^0$ is a canonical transformation from initial state to final state

$$x_{i\alpha} = x_{i\alpha}(x_{i\alpha}^0,\ p_{i\alpha}^0,\ t), \qquad p_{i\alpha} = p_{i\alpha}(x_{i\alpha}^0,\ p_{i\alpha}^0,\ t). \tag{2}$$

The solution (2) of the Hamilton equations (1) preserves the phase volume (Liouville's theorem [3]). The phase volume conservation condition has the following form [2]:

$$G^T J G = J, \qquad G = \frac{\partial(x_{i\alpha}, p_{i\alpha})}{\partial(x_{i\alpha}^0, p_{i\alpha}^0)}, \qquad J = \begin{Vmatrix} 0 & I_N \\ -I_N & 0 \end{Vmatrix}, \tag{3}$$

2021, **22** (2), 87–107. DOI: 10.26089/NumMet.v22r207

where G is Jacobi matrix, J is symplectic matrix, I_N is the identity matrix of size $N \times N$, upper index T denotes the transpose operation. It follows from (3) that the Jacobian transformation equals one: $|G| = 1$. For the subsequent discussion, let us rewrite the Hamiltonian equations (1) for the one-dimensional case in the form

$$dx_i/dt = p_i(t)/m, \quad dp_i/dt = f_i(x_i), \tag{4}$$

where $f_i(x_i)$ is the force acting on the i-th particle, $f_i(x_i) = -\partial V(x_i)/\partial x_i$, $i = 1, 2, \ldots, N$. Starting from here, we will omit the lower index i when discussing difference schemes for solving the system of ordinary differential equations (4).

3. Symplectic difference RKN schemes. The K-stage RKN scheme for the Hamiltonian equations (4) has the following form:

$$\begin{aligned} x^{(i)} &= x^n + h\alpha_i \frac{p^n}{m} + \frac{h^2}{m}\sum_{j=1}^{K} a_{ij} f(x^{(j)}), \\ x^{n+1} &= x^n + h\frac{p^n}{m} + \frac{h^2}{m}\sum_{j=1}^{K} \beta_j f(x^{(j)}), \\ p^{n+1} &= p^n + h\sum_{j=1}^{K} \gamma_j f(x^{(j)}), \end{aligned} \tag{5}$$

where h is the time step, n is the number of the time layer, $n = 0, 1, 2, \ldots$; $\alpha_i, \beta_i, \gamma_i$, $i = 1, \ldots, K$ are fixed parameters, $K \geqslant 1$.

Let us require that scheme (5) performs the canonical transformation $(x^n, p^n) \to (x^{n+1}, p^{n+1})$ at transition from temporal layer n to layer $n+1$. For this purpose it is necessary to impose the condition [3] on the Jacobi matrix G^{n+1} in accordance with (3)

$$G^{n+1,T} J G^{n+1} = J, \qquad G^{n+1} = \frac{\partial(x^{n+1}, p^{n+1})}{\partial(x^n, p^n)}, \qquad J = \begin{pmatrix} 0 & 1 \\ -1 & 0 \end{pmatrix}. \tag{6}$$

Condition (6) generates a class of explicit two-parameter RKN(α, γ) schemes, for which β_i, a_{ij} in (5) meet the conditions [11]

$$\beta_i = \gamma_i(1 - \alpha_i), \qquad a_{ij} = \begin{cases} 0, & \text{if } 1 \leqslant i \leqslant j \leqslant K, \\ \gamma_j(\alpha_i - \alpha_j), & \text{if } 1 \leqslant j < i \leqslant K. \end{cases} \tag{7}$$

There are no explicit Runge-Kutta schemes preserving the canonicity of transformation (6) [11].

Verlet [10] proposed a single-stage RKN scheme of the second-order accuracy for system (4). Ruth [5] proved for the first time that the Verlet scheme is symplectic (canonical) and discovered a three-stage RKN method of the third-order accuracy. A three-stage symplectic RKN-method of the fourth-order accuracy was obtained in [7]; two real symplectic four-stage schemes were also obtained in analytical form without using Gröbner bases. In [12], analytical expressions for $\alpha_i, \beta_i, \gamma_i$ ratios of the three-stage method were obtained, using Gröbner basis.

Let us describe the technique for determining the order of accuracy of the RKN scheme using the RKN scheme for calculating the momentum p^{n+1} at time $t_{n+1} = t_n + h$ as an example. We assume the value of p^n to be known. In each subsequent node t_{n+1}, the solution is calculated using the following formula: $p^{n+1} = p^n + \Delta p_{h,n}$. The formula for calculating $\Delta p_{h,n}$ depends on the number of stages K in the RKN scheme being considered and on the $3K$ variables $\alpha_i, \beta_i, \gamma_i$, $i = 1, \ldots, K$. On the other hand, one can easily obtain the "exact" formula for calculating the increment Δp by decomposing the value p^n into a truncated Tailor series: $\Delta p_n = p(t_n + h) - p(t_n) \approx \sum\limits_{j=1}^{N_T} \frac{h^j}{j!}\frac{d^j p(t_n)}{dt^j}$, where N_T is the given natural value, $N_T \geqslant K + 1$. If the difference $\delta p_n = \Delta p_n - \Delta p_{h,n}$ meets the condition $\delta p_n/h = O(h^\lambda)$, where $\lambda > 0$, then the RKN scheme has the order of accuracy $O(h^\lambda)$. λ degree is maximized by adjusting the parameters $\alpha_i, \beta_i, \gamma_i$ $(i = 1, \ldots, K)$ for each specific K.

3.1. One-stage RKN scheme. Let us assume $K = 1$ in (5) and find the highest possible order of accuracy for this scheme (Verlet scheme [10]) as applied to calculating the momentum p^{n+1} by varying the ratios α_1 and γ_1. Before citing the corresponding code fragments in the *Mathematica* language, let us explain the meaning of the notations used in this program:

$$\mathsf{ntayl} = N_T, \quad \mathsf{tn} = t_n, \quad \mathsf{pnew} = p^{n+1}, \quad \mathsf{u[t]} = \dot{x}(t), \quad \mathsf{dp} = \Delta p_n,$$

2021, **22** (2), 87–107. DOI: 10.26089/NumMet.v22r207

$$\mathsf{dph} = \Delta p_{h,n}, \quad \mathsf{errp} = \delta p_n, \quad \mathsf{a1} = \alpha_1, \quad \mathsf{g1} = \gamma_1.$$

First we calculate the "exact" decomposition of Δp_n (which corresponds to the variable dp in the *Mathematica* code fragment below):

```
pnew = Normal[ Series[ p[t], t, tn, ntayl] ] /. t -> tn + h;
dp = pnew - p[tn].
```

These commands produce the following expression for Δp_n:

$$\mathsf{dp} = \mathsf{hp'[tn]} + 1/2\mathsf{h}^2\mathsf{p''[tn]} + 1/6\mathsf{h}^3\mathsf{p}^{(3)}\mathsf{[tn]}.$$

To facilitate collecting like terms in the expression for δp_n, it helps to perform rather obvious transformations in the resulting expression, using the Hamiltonian equations (4):

$$p'(t_n) = f(x(t)), \quad p''(t_n) = f'(x(t))u(t), \quad p^{(3)}(t_n) = u^2(t)f''(x(t)) + f'(x(t))u'(t).$$

According to the Hamiltonian equations (4), calculating p^{n+1} requires the value of $x^{(1)}$. In our *Mathematica* program, it was calculated in symbolic form using the following function:

```
x1[t_] := x[t] + h*a1*u[t].
```

After that the value $\Delta p_{h,n}$ is calculated in symbolic form using the commands

```
ftayl1 = Normal[ Series[ f[y], y, y0, ntayl] ] /. {y -> x1[t], y0 -> x[t]};
dph = h*g1*ftayl1.
```

The value sought δp_n is calculated with this command: `errp = Simplify[dp - dph]`. As a result, the following expression for the error δp_n was obtained:

$$\delta p_n = hP_1 f(x) + \frac{h^2}{2} P_2 u(t) f'(x) + \frac{h^3}{6}[f(x)f'(x)/m + P_3 u^2 f''(x)].$$

Here P_1, P_2, P_3 are polynomials dependent on the parameters α_1, γ_1: $P_1 = 1 - \gamma_1$, $P_2 = 1 - 2\alpha_1\gamma_1$, $P_3 = 1 - 3\alpha_1^2\gamma_1$. As follows from these formulas, to ensure the second-order accuracy of the Verlet scheme, the parameters α_1, γ_1 need to be adjusted so that $P_1 = 0$, $P_2 = 0$. From these conditions we find: $\gamma_1 = 1$, $\alpha_1 = 1/2$. Given these parameters, the value of the P_3 ratio is different from zero: $P_3 = 1/4$.

Using similar symbolic calculations, the following expression for the error $\delta x_n = \Delta x_n - \Delta x_{h,n}$ is derived from the x^{n+1} calculation using the Verlet scheme:

$$\delta x_n = (h^2/2)R_2 f(x)/m + (h^3/6)\, R_3\, p(t)\, f'(x)/m^2. \tag{8}$$

Here R_2, R_3 are polynomials dependent on the parameters α_1, β_1: $R_2 = 1 - 2\beta_1$, $R_3 = 1 - 6\alpha_1\beta_1$. In order for the RKN scheme for x^{n+1} to have the same order of accuracy as the RKN-scheme for computing p^{n+1}, the equation $R_2 = 0$ must remain true for all the solutions of the polynomial system $P_1 = 0$, $P_2 = 0$. The *Mathematica* function PolynomialReduce[...] makes it possible to find an expression for a polynomial R_2 as a linear combination of given polynomials. In the case of polynomial R_2, the command PolynomialReduce[R2,{P2,P1}] produces the following result: $R_2 = 2P_1 - P_2$. In a similar manner, we find that $R_3 = 3P_2 - 2P_3$. The optimal values $\alpha_1 = 1/2$ and $\gamma_1 = 1$ were obtained above, based on the conditions $P_1 = 0$, $P_2 = 0$, which result in the equations $R_2 = 0$, $R_3 = -1/2$. Thus, the equation for $x(t)$ is also approximated by the Verlet scheme with the second-order accuracy.

3.2. Two-stage RKN scheme. In the case considered, we must assume $K = 2$ in (5). Performing symbolic calculations similarly to the case of the one-stage scheme, we arrive at the following expression for δp_n:

$$\delta p_n = hP_1 f(x) + \frac{h^2}{2} P_2 u f'(x) + \frac{h^3}{6m}\left[P_{31} f(x)f'(x) + P_{32} m u^2 f''(x)\right],$$

where

$$P_1 = 1 - \sum_{j=1}^{K} \gamma_j, \quad P_2 = 1 - 2\sum_{j=1}^{K} \alpha_j\gamma_j, \quad P_{31} = 1 - 6\sum_{i=1}^{K}\sum_{j=i+1}^{K} \gamma_i\gamma_j(\alpha_j - \alpha_i), \quad P_{32} = 1 - 3\sum_{j=1}^{K} \alpha_j^2\gamma_j. \tag{9}$$

A system of four nonlinear algebraic equations $P_1 = 0$, $P_2 = 0$, $P_{31} = 0$, $P_{32} = 0$ gives the following two solutions for parameters $\alpha_1, \alpha_2, \gamma_1, \gamma_2$: $\alpha_1 = (3 \pm \mathrm{i}\sqrt{3})/12$, $\alpha_2 = (9 \pm \mathrm{i}\sqrt{3})/12$, $\gamma_1 = (3 \pm \mathrm{i}\sqrt{3})/6$, $\gamma_2 = (3 \mp \mathrm{i}\sqrt{3})/6$. This means there are no real third-order accuracy schemes in this case. The choice of parameters $\alpha_1, \alpha_2, \gamma_1, \gamma_2$ from the conditions $P_1 = 0$, $P_2 = 0$ ensures second-order accuracy of the RKN scheme in question. These two

2021, **22** (2), 87–107. DOI: 10.26089/NumMet.v22r207

equations are linear with respect to γ_1, γ_2. Let us put them down as a system $V \cdot X = f$, where V is the Vandermonde matrix:

$$V = \begin{pmatrix} 1 & 1 \\ \alpha_1 & \alpha_2 \end{pmatrix}, \qquad X = \begin{pmatrix} \gamma_1 \\ \gamma_2 \end{pmatrix}, \qquad f = \begin{pmatrix} 1 \\ \frac{1}{2} \end{pmatrix}. \tag{10}$$

First let us consider the case where the determinant $\operatorname{Det} V = \alpha_2 - \alpha_1 = 0$. In this case we arrive from (10) to a one-parameter solution in the form $\gamma_2 = 1 - \gamma_1$, $\alpha_1 = \alpha_2 = 1/2$. Moreover, we obtain from (9): $P_{31} = 1$, $P_{32} = 1/4$, so that $144 \cdot (P_{31}^2 + P_{32}^2) = 144 \cdot \frac{17}{16} = 153$.

Let us now consider the case when $\alpha_1 \neq \alpha_2$. In this case, from the conditions $P_1 = 0$, $P_2 = 0$ it is easy to obtain the following two-parameter solution ensuring second-order accuracy of the two-stage RKN scheme:

$$\gamma_1 = (1 - 2\alpha_2)/\left[2(\alpha_1 - \alpha_2)\right], \qquad \gamma_2 = (2\alpha_1 - 1)/\left[2(\alpha_1 - \alpha_2)\right]. \tag{11}$$

In the theory of ordinary (non-symplectic) Runge-Kutta multistage schemes, it is common to find such scheme parameters (in the case in question, parameters α_1, α_2) that ensure a minimum of error terms, in this case with the order of smallness $O(h^3)$ [13]. Since both polynomials P_{31} and P_{32} depend on the parameters α_1, α_2, it makes sense to introduce the following quadratic functional:

$$F(\alpha_1, \alpha_2) = 144\left(P_{31}^2 + P_{32}^2\right) = \left[(\alpha_1(8 - 12\alpha_2) + 4\alpha_2 - 3)/(\alpha_1 - \alpha_2)\right]^2 + \left(\alpha_1(6\alpha_2 - 3) + 2 - 3\alpha_2\right)^2. \tag{12}$$

This expression is obtained by substituting formulas (11) into P_{31} and P_{32}. At the minimum point of function $F(\alpha_1, \alpha_2)$, the relations $\partial F(\alpha_1, \alpha_2)/\partial\alpha_l = 0$, $l = 1, 2$ must be true. The numerators of the resulting rational fractional expressions are as follows:

$$\begin{aligned} Q_1 = {} & -3 + 8\alpha_1 - 2\alpha_1^3 + 3\alpha_1^4 + 16\alpha_2 - 44\alpha_1\alpha_2 + 6\alpha_1^2\alpha_2 - 2\alpha_1^3\,\alpha_2 - 12\alpha_1^4\,\alpha_2 - 28\alpha_2^2 + 74\alpha_1\alpha_2^2 - 12\alpha_1^2\,\alpha_2^2 + \\ & + 30\alpha_1^3\,\alpha_2^2 + 12\alpha_1^4\,\alpha_2^2 + 18\alpha_2^3 - 30\alpha_1\alpha_2^3 - 18\alpha_1^2\alpha_2^3 - 36\alpha_1^3\alpha_2^3 - 7\alpha_2^4 - 6\alpha_1\alpha_2^4 + 36\alpha_1^2\alpha_2^4 + 6\alpha_2^5 - 12\alpha_1\alpha_2^5, \\ Q_2 = {} & 3 - 20\alpha_1 + 44\alpha_1^2 - 34\alpha_1^3 + 7\alpha_1^4 - 6\alpha_1^5 - 4\alpha_2 + 28\alpha_1\alpha_2 - 58\alpha_1^2\alpha_2 + 30\alpha_1^3\alpha_2 + 6\alpha_1^4\alpha_2 + 12\alpha_1^5\alpha_2 - \\ & - 6\alpha_1\alpha_2^2 + 12\alpha_1^2\alpha_2^2 + 18\alpha_1^3\alpha_2^2 - 36\alpha_1^4\alpha_2^2 + 2\alpha_2^3 + 2\alpha_1\alpha_2^3 - 30\alpha_1^2\alpha_2^3 + 36\alpha_1^3\alpha_2^3 - 3\alpha_2^4 + 12\alpha_1\alpha_2^4 - 12\alpha_1^2\alpha_2^4\,. \end{aligned}$$

The solution of the system $Q_1 = 0$, $Q_2 = 0$ was found using the Gröbner basis. For this, we used the GroebnerBasis[{Q1,Q2}, {a1,a2}] function that is built in the *Mathematica* software package. Here a1= α_1, a2= α_2. It turned out that the Gröbner basis consists of four polynomials, of which the first three are reducible, as we discovered using the Factor[...] built-in function of the software package used:

$$G_1 = \left(-1 + 2\,\alpha_2\right)^9 \left(15 + 2\,\alpha_2\right)\left(7 - 18\,\alpha_2 + 12\,\alpha_2^2\right)\left(-3 + 7\,\alpha_2 - 9\,\alpha_2^2 + 6\,\alpha_2^3\right),$$

$$\begin{aligned} G_2 = {} & -\big((-1 + 2\,\alpha_2)^2\,(-782292886326335781 + 84791412129792\alpha_1 + 13518496830811327517\,\alpha_2 - \\ & - 105687991753500756247\,\alpha_2^2 + 494822074007590215378\,\alpha_2^3 - 154776110385750120352 4\,\alpha_2^4 + \\ & + 341340314160887430428 8\,\alpha_2^5 - 544502718046385732380 8\,\alpha_2^6 + 630546622313818163897 6\,\alpha_2^7 - \\ & - 518308024999394690675 2\,\alpha_2^8 + 282869138372866177766 4\,\alpha_2^9 - 85536820935690632956\,\alpha_2^{10} + \\ & + 51213785868624923136\,\alpha_2^{11} + 30677230391300103168\,\alpha_2^{12})\big), \end{aligned}$$

$$\begin{aligned} G_3 = {} & (-1 + 2\,\alpha_2)\,\big(138375335965152699 + 15898389774336\,\alpha_1 - 31796779548672\,\alpha_1^2 + \\ & + 21197853032448\,\alpha_1^3 - 2643993979226915641\,\alpha_2 + 23052596110039882255\,\alpha_2^2 - \\ & - 12152354661541497625 6\,\alpha_2^3 + 432612502387510859032\,\alpha_2^4 - 109959756543894802722 4\,\alpha_2^5 + \\ & + 205446656380383777961 6\,\alpha_2^6 - 285290452325521955392 0\,\alpha_2^7 + 292515969259528388838 4\,\alpha_2^8 - \\ & - 214798750702410340403 2\,\alpha_2^9 + 104855522943601326873 6\,\alpha_2^{10} - 279638949859173402624\,\alpha_2^{11} + \\ & + 10628391427610609664\,\alpha_2^{12} + 9693762746554238976\,\alpha_2^{13}\big), \end{aligned} \tag{13}$$

$$\begin{aligned} G_4 = {} & -6378840443102352741 + 105989265162240\,\alpha_1 - 402759207616512\,\alpha_1^2 + \\ & + 423957060648960\,\alpha_1^3 - 42395706064896\,\alpha_1^4 + 134645083671004390385\,\alpha_2 + \\ & + 339165648519168\,\alpha_1\alpha_2 - 339165648519168\,\alpha_1^2\alpha_2 - 130655337147154022780 7\,\alpha_2^2 + \\ & + 772838546356896718288 2\,\alpha_2^3 - 311522922249761136552 72\,\alpha_2^4 + 905955462301405829338 80\,\alpha_2^5 - \\ & - 196140611828089238849712\,\alpha_2^6 + 321032661222529636238400\,\alpha_2^7 - \\ & - 398020598628892865210880\,\alpha_2^8 + 368863060403416970198016\,\alpha_2^9 - \\ & - 246489793612098299292928\,\alpha_2^{10} + 109621999423243454814720\,\alpha_2^{11} - \\ & - 262875572351235447459 84\,\alpha_2^{12} + 533712029766168066048\,\alpha_2^{13} + 894285199654734163968\,\alpha_2^{14}\,. \end{aligned}$$

2021, **22** (2), 87–107. DOI: 10.26089/NumMet.v22r207

Equation $G_1 = 0$ has a total of 15 solutions, counted together with their multiplicities. The equation $-1+2\alpha_2 = 0$ gives the root $\alpha_2 = 1/2$. By substituting this value into (13), we obtain:

$$G_4 = -2649731629056\,(-17 + 2\alpha_1)(-1 + 2\alpha_1)^3.$$

From this we derive that the root $\alpha_2 = 1/2$ corresponds to the following two roots α_1: $\alpha_1 = 17/2$ and $\alpha_1 = 1/2$. The pair of roots $\alpha_1 = \alpha_2 = 1/2$ has already been obtained above, in the singular case where the Vandermonde determinant $\operatorname{Det} V$ turns to zero.

The second polynomial multiplier in G_1 gives a single root $\alpha_2 = -15/2$. By substituting this value into G_4, we obtain the following factorized polynomial:

$$-2649731629056\,(-1 + 2\alpha_1)^2\,(-239 - 36\,\alpha_1 + 4\alpha_1^2).$$

The value $\alpha_1 = 1/2$ is one of its roots. Note that $F(1/2, -15/2) = 17/4$. The equation $4\alpha_1^2 - 36\alpha_1 - 239 = 0$ has two roots: $\alpha_1^{(4),(5)} = \dfrac{1}{2}\left(9 \pm 8\sqrt{5}\right)$. The third polynomial multiplier in G_1 gives two complex roots. The fourth multiplier in G_1 leads to the equation $6\alpha_2^3 - 9\alpha_2^2 + 7\alpha_2 - 3 = 0$, which has one real solution $\alpha_2 = \dfrac{1}{6}\left(3 - \dfrac{5}{z} + z\right) \approx 0.8207801830727278$, where $z = \left(18 + \sqrt{449}\right)^{\frac{1}{3}}$.

Substituting this solution into G_4, we obtain the fourth-degree equation for finding α_1, which is not given here due to its bulkiness. It has two real roots: $\alpha_1^{(6)} = 0.1792198169272722$ and $\alpha_1^{(7)} = 8.1664593831518564$. Thus, we found seven real solutions. The value of function F is shown below to the right of each α_1, α_2 value pair:

$$\begin{gathered}
\left(\alpha_1^{(1)} = \frac{1}{2},\ \alpha_2^{(1)} = \frac{1}{2},\ 153\right), \qquad \left(\alpha_1^{(2)} = \frac{17}{2},\ \alpha_2^{(2)} = \frac{1}{2},\ \frac{17}{4}\right), \qquad \left(\alpha_1^{(3)} = \frac{1}{2},\ \alpha_2^{(3)} = -\frac{15}{2},\ \frac{17}{4}\right), \\
\left(\alpha_1^{(4)} = \frac{1}{2}(9 - 8\sqrt{5}),\ \alpha_2^{(4)} = -\frac{15}{2},\ 80071.2\right), \qquad \left(\alpha_1^{(5)} = \frac{1}{2}(9 + 8\sqrt{5}),\ \alpha_2^{(5)} = -\frac{15}{2},\ 389185\right), \\
\left(\alpha_1^{(6)} = 0.1792198169272722,\ \alpha_2^{(6)} = 0.8207801830727278,\ 0.019455592\right), \\
\left(\alpha_1^{(7)} = 8.1664593831518564,\ \alpha_2^{(7)} = 0.8207801830727278,\ 236.8001073\right).
\end{gathered} \tag{14}$$

It follows that the values $\alpha_1^{(6)}$ and $\alpha_2^{(6)}$ are the optimal values at which the functional (12) reaches its minimum. Let us prove that the equation $\alpha_1^{(6)} + \alpha_2^{(6)} = 1.$ is true. To do this, we replace the value of α_1 in G_4 by the formula: $\alpha_1 = 1 - \alpha_2$. We arrive at the following polynomial with one variable:

$$\begin{gathered}
G_4(1-\alpha_2, \alpha_2) = (-1+2\,\alpha_2)^3\left(-3+7\,\alpha_2-9\,\alpha_2^2+6\,\alpha_2^3\right)\left(-2126251883896740983+2716279460479274 9766\,\alpha_2-\right. \\
-14749954618310618 5992\,\alpha_2^2 + 4401742561132686 36584\,\alpha_2^3 - 7756251587417784 88992\,\alpha_2^4+ \\
+7970313429134098 08288\,\alpha_2^5 - 4242508891838991 40736\,\alpha_2^6+ \\
\left.+6701182559854938 6624\,\alpha_2^7 + 1863094165947362 8416\,\alpha_2^8\right).
\end{gathered}$$

Using the expression $\alpha_2 = \dfrac{1}{6}\left[3 - \dfrac{5}{z} + z\right]$, where $z = \left(18 + \sqrt{449}\right)^{\frac{1}{3}}$, we obtain: $G_4(1 - \alpha_2, \alpha_2) = 0$.

Using symbolic calculations similar to the case of the Verlet scheme, the expression for the error δx_n is found in the form (8), where $R_2 = 2P_1 - P_2$, $R_3 = 3P_2 - 2P_{32}$. Let us use the expressions from (7) for β_1 and β_2 and substitute R_2, R_3 with formulas (11) obtained above from the second-order accuracy requirement of the RKN scheme in question for momentum p^{n+1}. The result is: $R_2 = 0$, $R_3 = -2 + \alpha_1(3 - 6\alpha_2) + 3\alpha_2$. Now let us substitute in R_3 the values $\left(\alpha_1^{(l)},\ \alpha_2^{(l)}\right)$ from (14), $l = 1, \ldots, 7$. Let us denote the corresponding numerical values of the value R_3 through $R_3^{(l)}$. It turns out that $R_3^{(1)} = R_3^{(2)} = R_3^{(3)} = -\dfrac{1}{2}$, $R_3^{(4)} = -\dfrac{49}{2} + 24\left(9 - 8\sqrt{5}\right) \approx -237.825$, $R_3^{(5)} = -\dfrac{49}{2} + 24\left(9 + 8\sqrt{5}\right) \approx 620.825$, $R_3^{(6)} = (25 - 13z^2 + z^4)/(6z^2) \approx 0.11740$, where $z = \left(18 + \sqrt{449}\right)^{\frac{1}{3}}$, $R_3^{(7)} \approx -15.2555$. It follows that the value $R_3^{(6)}$ is the smallest absolute value among the seven values $R_3^{(l)}$, $l = 1, \ldots, 7$, where $|R_3^{(l)}|/R_3^{(6)} = 4.259$ at $l \leqslant 3$. Thus, the point $\left(\alpha_1^{(6)},\ \alpha_2^{(6)}\right)$ is optimal

2021, **22** (2), 87–107. DOI: 10.26089/NumMet.v22r207

in terms of accuracy also when calculating x^{n+1} using the two-stage RKN scheme. We should also note that the values of $R_3^{(l)}$ at $l \leqslant 3$ match the value of R_3 obtained in the previous section for the one-stage RKN scheme. Therefore, when using the point $\left(\alpha_1^{(6)},\ \alpha_2^{(6)}\right)$ in the two-stage scheme, a higher accuracy of the numerical solution should be expected than in the case of the Verlet scheme.

The general conclusion is that the two-stage scheme in question has only the second-order accuracy, and cannot be advanced to third-order accuracy.

3.3. A three-stage RKN scheme. Assuming $K = 3$ in (5) and performing symbolic calculations similar to the case of the two-stage scheme, we obtain the expression for δp_n in the form

$$\begin{aligned}\delta p_{n,3} = {} & hP_1 f(x) + (h^2/2)P_2 u f'(x) + (h^3/(6m))[P_{31} f(x) f'(x) + P_{32} m u^2 f''(x)] + \\ & + (h^4 u)/(24m)\{P_{41} \cdot [f'(x)]^2 + 3P_{42} f(x) f''(x) + P_{43} m u^2 f^{(3)}(x)\} + \\ & + [h^5/(120m^2)](3P_{51} f^2(x) f''(x) + f(x)(P_{52} \cdot [f'(x)]^2 + 6P_{53} m u^2 f^{(3)}(x)) + \\ & + m u^2 (5P_{54} f'(x) f''(x) + P_{55} m u^2 f^{(4)}(x)),\end{aligned} \tag{15}$$

where the polynomials P_1, P_2, P_{31}, P_{32} are described by formulas (9);

$$\begin{aligned}
P_{41} &= 1 - 24 \sum_{i=1}^{K} \sum_{j=i+1}^{K} \gamma_i \gamma_j \alpha_i (\alpha_j - \alpha_i), \\
P_{42} &= 1 - 8 \sum_{i=1}^{K} \sum_{j=i+1}^{K} \gamma_i \gamma_j \alpha_j (\alpha_j - \alpha_i), \\
P_{43} &= 1 - 4 \sum_{j=1}^{K} \alpha_j^3 \gamma_j, \\
P_{51} &= 1 - 20 \sum_{i=1}^{K} \sum_{j=i+1}^{K} \sum_{l=j+1}^{K} \gamma_i \gamma_j \gamma_l (\alpha_j - \alpha_i)(\alpha_i - \alpha_l), \\
P_{52} &= 1 - 120 \sum_{i=1}^{K} \sum_{j=i+1}^{K} \sum_{l=j+1}^{K} \gamma_i \gamma_j \gamma_l (\alpha_j - \alpha_i)(\alpha_j - \alpha_l), \\
P_{53} &= 1 - 10 \sum_{i=1}^{K} \sum_{j=i+1}^{K} \gamma_i \gamma_j \alpha_i^2 (\alpha_i - \alpha_j), \\
P_{54} &= 1 - 12 \sum_{i=1}^{K} \sum_{j=i+1}^{K} \gamma_i \gamma_j \alpha_j^2 (\alpha_i - \alpha_j), \\
P_{55} &= 1 - 5 \sum_{j=1}^{K} \alpha_j^4 \gamma_j.
\end{aligned} \tag{16}$$

This RKN scheme was investigated in [12] using *Maple 12* software package and Gröbner bases. In Section 5, we will compare the three-stage scheme in terms of accuracy with the other four schemes, so below we give three sets of parameters α_l, γ_l, $l = 1, 2, 3$, which were derived in [12] from the fourth-order accuracy requirement of the three-stage scheme in question:

$$\alpha_1 = \frac{3 \mp z}{6}, \quad \alpha_2 = \frac{3 \pm z}{6}, \quad \alpha_3 = \frac{3 \mp z}{6}, \quad \gamma_1 = \frac{3 \pm 2z}{12}, \quad \gamma_2 = \frac{1}{2}, \quad \gamma_3 = \frac{3 \mp 2z}{12}, \tag{17}$$

where $z = \sqrt{3}$. Let us call the scheme with the upper "+" and "−" signs in (17) the RKN34A scheme. The scheme with the lower "+" and "−" signs in (17) will be called the RKN34B scheme. The third set of parameters is as follows ($\zeta = 2^{1/3}$):

$$\begin{aligned}
\alpha_1 &= \frac{\zeta}{6} + \frac{\zeta^2}{12} + \frac{1}{3}, & \alpha_2 &= \frac{1}{2}, & \alpha_3 &= \frac{2}{3} - \frac{\zeta}{6} - \frac{\zeta^2}{12}, \\
\gamma_1 &= \frac{\zeta}{3} + \frac{\zeta^2}{6} + \frac{2}{3}, & \gamma_2 &= -\frac{2\zeta}{3} - \frac{\zeta^2}{3} - \frac{1}{3}, & \gamma_3 &= \frac{\zeta}{3} + \frac{\zeta^2}{6} + \frac{2}{3}.
\end{aligned} \tag{18}$$

We call this scheme the RKN34C scheme.

2021, **22** (2), 87–107. DOI: 10.26089/NumMet.v22r207

Let us find out which of the three RKN schemes RKN34A, RKN34B, RKN34C produces the best accuracy. To do this, we compute the weighted RMS value of the five polynomials P_{5j}, $j = 1, \ldots, 5$:

$$P_{5,\,\mathrm{rms}} = \sqrt{\frac{1}{5}\sum_{j=1}^{5}(\sigma_j P_{5j})^2}. \tag{19}$$

Here $\sigma_1, \ldots, \sigma_5$ are the multipliers of polynomials P_{5j} in (15); they are not dependent on the specifics of the problem being solved; $\sigma_1 = 3$, $\sigma_2 = 1$, $\sigma_3 = 6$, $\sigma_4 = 5$, $\sigma_5 = 1$. Let us denote the values of polynomial (19) for the RKN34A, RKN34B, RKN34C schemes as $P_{5\mathrm{A,rms}}$, $P_{5\mathrm{B,rms}}$, $P_{5\mathrm{C,rms}}$, respectively. The following results are produced:

$$P_{5\mathrm{A,rms}} = P_{5\mathrm{B,rms}} = \frac{1}{72}\sqrt{\frac{5953}{5}} \approx 0.47924, \quad P_{5\mathrm{C,rms}} = \frac{1}{288}\left[\frac{5560768}{5} + 886480\zeta + 698117\zeta^2\right]^{\frac{1}{2}} \approx 6.3431, \tag{20}$$

where $\zeta = 2^{1/3}$. It follows that RKN34A and RKN34B schemes are the most accurate of the three three-stage fourth-order accuracy schemes.

Let us denote the error obtained when calculating the coordinate of x^{n+1} particle using the three-stage RKN scheme by $\delta x_{n,3}$. This error is found using symbolic calculations similar to the two-stage RKN scheme case, and has the following form:

$$\begin{aligned}\delta x_{n,3} = \delta x_n + \frac{h^4}{24m^3}\left[R_{41} m f(x) f'(x) + R_{42} p^2 f''(x)\right] + \\ + \frac{h^5 p(t)}{120m^4}\left\{R_{51} m [f'(x)]^2 + 3R_{52} m f(x) f''(x) + R_{53} p^2 f^{(3)}(x)\right\}.\end{aligned} \tag{21}$$

Here, δx_n is calculated using formula (8), in which $R_2 = 2P_1 - P_2$, $R_3 = 3P_2 - 2P_{32}$, and polynomials P_1, P_2, P_{31}, P_{32} are calculated using formula (9) with $K = 3$. Further, $R_{41} = 4P_{31} - 3P_{42}$, $R_{42} = 4P_{32} - 3P_{43}$.

From the formulas for R_2, R_3, R_{41}, R_{42}, it follows that the value x^{n+1} is also found with the fourth-order accuracy using the three-stage RKN scheme. The polynomials R_{51}, R_{52}, R_{53} have the following form:

$$\begin{aligned} R_{51} &= 1 - 120\sum_{i=1}^{K}\sum_{j=i+1}^{K}(\alpha_j - \alpha_i)\gamma_i\alpha_i\beta_j, \\ R_{52} &= 1 - 40\sum_{i=1}^{K}\sum_{j=i+1}^{K}(\alpha_j - \alpha_i)\gamma_i\alpha_j\beta_j, \\ R_{53} &= 1 - 20\sum_{i=1}^{K}\alpha_i^3\beta_i. \end{aligned} \tag{22}$$

3.4. A four-stage RKN scheme. Assuming $K = 4$ in (5) and performing symbolic calculations similar to the case of the three-stage scheme, we obtain the expression for δp_n in the form (15), where the expressions for P_1, P_2, P_{31}, P_{32}, P_{41}, P_{42}, P_{43}, P_{51}, P_{52}, P_{53}, P_{54}, P_{55} match the formulas (9), (16) at $K = 4$. The

```
GroebnerBasis[{P1, P2, P31, P32, P41, P42, P43, P51, P52, P53, P54, P55}, {a1, a2, a3, a4, g1, g2, g3, g4}]
```

command produces the following output: $\{1\}$. According to the Hilbert's theorem on zeros [14], if the ideal is $\{1\}$, then 12 polynomials $P_1, \ldots, P_{55}$ have no common zero values. Hence we conclude there are no four-stage schemes of the fifth-order accuracy.

The system of equations $P_1 = 0$, $P_2 = 0$, $P_{32} = 0$, $P_{43} = 0$ is linear relative to γ_i, $i = 1, \ldots, 4$. Its matrix is a Vandermonde matrix V of size 4×4, and

$$\mathrm{Det}\, V = (\alpha_1 - \alpha_2)(\alpha_1 - \alpha_3)(\alpha_1 - \alpha_4)(\alpha_2 - \alpha_3)(\alpha_2 - \alpha_4)(\alpha_3 - \alpha_4).$$

Using Gröbner bases, all six cases of this determinant turning to zero were considered, and 20 real schemes of fourth-order accuracy were discovered. For each scheme, the weighted RMS value of the five polynomials P_{5j}, $j = 1, \ldots, 5$ was calculated, similar to (19):

$$P^{(l)}_{5,\,\mathrm{rms}} = \sqrt{\frac{1}{5}\sum_{j=1}^{5}(\sigma_j P_{5j})^2}, \quad l = 1, \ldots, 20.$$

2021, **22** (2), 87–107. DOI: 10.26089/NumMet.v22r207

Next, the case of a non-zero Vandermonde determinant was considered. Applied molecular dynamics problems are non-linear, so they have to be solved using numerical methods, in particular, RKN-methods. To implement these methods programmatically it is sufficient to set the parameters α_j, γ_j $(j = 1, \ldots, K)$ as floating-point numbers in machine representation. The problem of finding a solution to a polynomial system that satisfies the aforementioned parameters can be formulated as a problem of numerical minimization of a target function representing a sum total of squared left-hand sides of the polynomial system being solved.

The progress in numerical solution of optimization problems achieved over the last decades makes it possible to approximate a numerical solution to the optimization problems within acceptable machine time, at sufficient accuracy for practical applications. The *Mathematica* function NMinimize[...] makes it possible to find the minimum of a multivariate function.

Let us assume $X = (\alpha_1, \alpha_2, \alpha_3, \alpha_4, \gamma_1, \gamma_2, \gamma_3, \gamma_4)$. We proceed by introducing a non-negative target function

$$P(X) = P_1^2 + P_2^2 + P_{31}^2 + P_{32}^2 + P_{41}^2 + P_{42}^2 + P_{43}^2. \tag{23}$$

Further, let $\Omega_{8\mathrm{d}}$ be a hypercube with $2r$ edge length in an eight-dimensional Euclidean space of X-points, $\Omega_{8\mathrm{d}} = \{(\alpha_1, \alpha_2, \alpha_3, \alpha_4, \gamma_1, \gamma_2, \gamma_3, \gamma_4) \,|\, -r \leqslant \alpha_j \leqslant r, \quad -r \leqslant \gamma_j \leqslant r, \quad j = 1, \ldots, 4\}$. We will seek a solution to the following numerical minimization problem: finding $\min_{X \in \Omega_{8\mathrm{d}}} P(X)$.

In the case of nonlinear target function, the NMinimize[...] function in *Mathematica* uses the minimization algorithm proposed in [15]. Let us assume that X^* is an approximate solution of the minimization problem for function (23) in hypercube $\Omega_{8\mathrm{d}}$, if $|P(X^*)| < 10^{-30}$. Then the RMS value of the functions $P_1, \ldots, P_{43}$ meets the inequality condition $\sqrt{\left(P_1^2 + \cdots + P_{43}^2\right)/7} < \dfrac{10^{-15}}{\sqrt{7}} \approx 0.378 \cdot 10^{-15}$, i.e., it will stay at the level of machine rounding errors at double-precision computation upon executing the machine code generated by the FORTRAN program translator. Thus, the accuracy observed in determining the components of vector X^* is sufficient for numerical solution of molecular dynamics problems by means of RKN schemes.

In order to obtain several solutions to the minimization problem of function (23) in one run of the *Mathematica* program, several initial X-points were set in the $\Omega_{8\mathrm{d}}$ region. The number of points was set by the user. The point coordinates were set using the pseudorandom number generator built into the *Mathematica* software.

By placing 1000 initial points randomly in $\Omega_{8\mathrm{d}}$, 164 numerical solutions of the polynomial system in question were obtained. Of these, we selected only the solutions in which the value $P_{5,\mathrm{rms}}$ is smaller than the lowest value obtained when considering all special cases of the Vandermond determinant turning to zero. The number of these solutions is 21. Of these, four solutions are presented in Table 1 in ascending order of the corresponding values of $P_{5,\mathrm{rms}}^{(l)}$. It turned out that in the general case, when $\mathrm{Det}V \neq 0$, it is possible to obtain schemes that have more than half as low $P_{5,\mathrm{rms}}^{(l)}$ values than in the cases of $\mathrm{Det}V = 0$.

Table 1. Parameter values of the schemes RKN4-la, $l = 1, \ldots, 4$, at $\mathrm{Det}\, V \neq 0$

Method	α_j	γ_j	$P_{5,\mathrm{rms}}^{(l)}$	κ_{cr}
1a	−0.163552401143382292	0.048726380769174189	0.1450	2.601107169201
	0.315379254000269726	0.604671155309221442		
	0.849651865097469039	0.377059806193216329		
	0.101814165555907346	−0.030457342271611940		
2a	−0.132366908603509081	0.050382034698121490	0.1659	2.853927732257
	0.554050453573154522	−0.106956632411513153		
	0.337015545852672127	0.632484935164970730		
	0.831831238456345323	0.424089662548420954		
3a	0.168126182298635241	0.419065819011724183	0.1676	2.855254281741
	0.636979619359235749	0.421942016918863572		
	0.922878504633673047	0.176843502495841326		
	0.136094487172141509	−0.017851338426429109		
4a	0.073135959738290263	0.179911393946207976	0.1763	2.8424607874720
	0.757772082233232225	−0.041533676753871755		
	0.377483410023031707	0.436525266982659255		
	0.831654913466108980	0.425097015825004532		

2021, **22** (2), 87–107. DOI: 10.26089/NumMet.v22r207

Let us use $\delta x_{n,4}$ to denote the error obtained when calculating the coordinates x^{n+1} of a particle using the four-step RKN scheme. This error is found using symbolic calculations similar to the three-stage RKN scheme case, and is expressed using the formula (21), in which one must assume that $K = 4$. Next, $R_2 = 2P_1 - P_2$, $R_3 = 3P_2 - 2P_{32}$, $R_{41} = 4P_{31} - 3P_{42}$, $R_{42} = 4P_{32} - 3P_{43}$, $R_{52} = 5P_{42} - 4P_{53}$, $R_{53} = 5P_{43} - 4P_{55}$, $R_{51} = 5(1-\alpha_2)P_{41} + r_1P_2 + r_2P_{32} + r_3$, where $r_1 = 60(\alpha_2\alpha_3\gamma_3 - \alpha_3^2\gamma_3 + \alpha_2\alpha_4\gamma_4 - \alpha_4^2\gamma_4)$, $r_2 = 40(\alpha_2\gamma_3 - \alpha_3\gamma_3 + \alpha_2\gamma_4 - \alpha_4\gamma_4)$, $r_3 = -4 + 5(\alpha_2 + 8\alpha_2\gamma_3 - 8\alpha_3\gamma_3 - 12\alpha_2\alpha_3\gamma_3 + 12\alpha_3^2\gamma_3 - 4((\alpha_2 - \alpha_4)(3\alpha_4 - 2) + 6(\alpha_2 - \alpha_3)\alpha_4(\alpha_4 - \alpha_3)\gamma_3)\gamma_4)$. If we substitute the polynomial system solution $\langle P_1 = 0, P_2 = 0, P_{31} = 0, P_{32} = 0, P_{41} = 0, P_{42} = 0, P_{43} = 0\rangle$, in the expressions for R_{51}, R_{52}, R_{53}, we obtain: $R_{51} = r_3$, $R_{52} = -4P_{53}$, $R_{53} = -4P_{55}$. It follows that the equation for $x(t)$ is also approximated by the RKN4 scheme with the fourth-order accuracy.

3.5. A five-stage RKN scheme. When $K = 5$ in (5), the expression for δp_n, taking into account (15), looks as follows:

$$\delta p_n = \delta p_{n,3} + \left[h^6u/(720m^2)\right]\Big\{\left[f'(x)\right]^3 + 15P_{61}f^2(x)f^{(3)}(x) - f'(x)\left[P_{62}f(x)f''(x) + P_{63}mu^2f^{(3)}(x)\right] + \\ + mu^2\left[5P_{64}\left(f''(x)\right)^2 + 10P_{65}f(x)f^{(4)}(x) + mP_{66}u^2f^{(5)}(x)\right]\Big\}, \tag{24}$$

where the polynomials P_1, P_2, P_{31}, P_{32}, P_{41}, P_{42}, P_{43}, P_{51}–P_{55} are described by formulas (9) and (16) at $K = 5$. Here are the expressions for the polynomials $P_{61}, \ldots, P_{66}$:

$$P_{61} = 1 - 24\left[\sum_{i=1}^{K}\sum_{j=i+1}^{K}\gamma_i^2\gamma_j\alpha_j(\alpha_i - \alpha_j)^2 + 2\sum_{i=1}^{K}\sum_{j=i+1}^{K}\sum_{l=j+1}^{K}\gamma_i\gamma_j\gamma_l\alpha_l(\alpha_i - \alpha_l)(\alpha_j - \alpha_l)\right],$$

$$P_{62} = 18 - 720\left[\sum_{i=1}^{K}\sum_{j=i+1}^{K}\gamma_i^2\gamma_j\alpha_i(\alpha_i - \alpha_j)^2 + \sum_{i=1}^{K}\sum_{j=i+1}^{K}\sum_{l=j+1}^{K}\gamma_i\gamma_j\gamma_l(\alpha_j - \alpha_l)\left[(\alpha_i^2 - \alpha_j^2) + 2\alpha_j(\alpha_i - \alpha_l)\right]\right],$$

$$P_{63} = 11 - 120\left[\sum_{i=1}^{K}\sum_{j=i+1}^{K}\gamma_i\gamma_j\alpha_i(\alpha_j - \alpha_i)(\alpha_i^2 + 3\alpha_j^2)\right], \tag{25}$$

$$P_{64} = 1 - 72\sum_{i=1}^{K}\sum_{j=i+1}^{K}\gamma_i\gamma_j\alpha_i^2\alpha_j(\alpha_j - \alpha_i),$$

$$P_{65} = 1 - 12\sum_{i=1}^{K}\sum_{j=i+1}^{K}\alpha_j^3\gamma_i\gamma_j(\alpha_j - \alpha_i),$$

$$P_{66} = 1 - 6\sum_{j=1}^{K}\alpha_j^5\gamma_j.$$

It was shown in [16, 17] that the conditions $P_{41} = 0$, $P_{52} = 0$ are redundant. In [16], the numerical values of the parameters α_i, γ_i $(i = 1, \ldots, 5)$ were found by numerical calculation with an error not exceeding 10^{-10}. As a result, four real methods were obtained [16, Table 1].

To determine which of the four methods is the most accurate, we calculated the weighed RMS numerical values of

$$P_{6,\,\mathrm{rms}} = \sqrt{\frac{1}{7}\left(1 + \sum_{j=1}^{6}(\sigma_jP_{6j})^2\right)} \tag{26}$$

for all four RKN methods of the fifth-order accuracy, where $\sigma_1 = 15$, $\sigma_2 = \sigma_3 = -1$, $\sigma_4 = 5$, $\sigma_5 = 10$, $\sigma_6 = 1$ in accordance with (24). It was found that $P_{6,\,\mathrm{rms}} \approx 11.33081$ for methods 1 and 3; $P_{6,\,\mathrm{rms}} \approx 7.11113$ for methods 2 and 4. The matching values (26) for pairs 1, 3 and 2, 4 is not accidental: as explained in [16], method 3 is conjugate to method 1 and method 4 is conjugate to method 2 [16, Table 1]. The conjugate method is obtained by replacing h, x^n, u^n, with $-h$, x^{n+1}, u^{n+1}, respectively.

As shown above, we used the NMinimize[...] function in *Mathematica* to obtain a large number of real solutions to a polynomial system corresponding to the RKN4 scheme. We use this function in a similar manner to find new real solutions of the polynomial system corresponding to the RKN5 scheme. Assume $X = (\alpha_1, \alpha_2, \alpha_3, \alpha_4, \alpha_5, \gamma_1, \gamma_2, \gamma_3, \gamma_4, \gamma_5)$. Let us introduce a non-negative target function $P(X) =$

2021, **22** (2), 87–107. DOI: 10.26089/NumMet.v22r207

$P_1^2 + P_2^2 + P_{31}^2 + P_{32}^2 + P_{42}^2 + P_{43}^2 + P_{51}^2 + P_{53}^2 + P_{54}^2 + P_{55}^2$. Further, let $\Omega_{10\mathrm{d}}$ be a rectangular parallelepiped in the ten-dimensional Euclidean space of X-points, $\Omega_{10\mathrm{d}} = \{(\alpha_1, \alpha_2, \alpha_3, \alpha_4, \alpha_5, \gamma_1, \gamma_2, \gamma_3, \gamma_4, \gamma_5) \big| -r_1 \leqslant \alpha_j \leqslant r_1, -r_2 \leqslant \gamma_j \leqslant r_2,\ j = 1, \ldots, 5\}$. Here r_1, r_2 are user-defined positive constants defining the lengths of the parallelepiped's edges. We will seek a solution to the following numerical minimization problem: finding $\min_{X \in \Omega_{10\mathrm{d}}} P(X)$.

The smaller the r_1, r_2 values, the fewer iterations are required to obtain a solution with machine accuracy. Given the results of [16], we set $r_1 = 1.2$, $r_2 = 2.0$. The minimization problem in question was solved numerically using the NMinimize[...] function in *Mathematica*, in a manner quite similar to the case of eight-dimensional space. As in the case of the four-stage RKN scheme, an approximate solution of the problem in question was defined as the solution satisfying the inequality $|P(X)| < 10^{-30}$.

By placing $2{\cdot}10^4$ starting points randomly in $\Omega_{10\mathrm{d}}$, three numerical solutions of the polynomial system in question were obtained. They are presented in Table 2 in ascending order of the respective values of $P^{(l)}_{6,\mathrm{rms}}$. As can be seen from this table, the values of $P^{(l)}_{6,\mathrm{rms}}$ are much smaller than in methods 1–4 of [16].

Further, Table 3 shows that the values $|P_1(X)|, |P_2(X)|, \ldots, |P_{55}(X)|$ in case of methods 5, 6, 7 lie within the range of 0 to $3.1{\cdot}10^{-15}$, and in the case of methods from [16] they lie, in descending order, in the range of $O(10^{-15})$ to $O(10^{-11})$, as shown in Table 4.

Let us use $\delta x_{n,5}$ to denote the error obtained when calculating the coordinate x^{n+1} of a particle using the five-step RKN scheme. This error is found using symbolic calculations similar to those in the three-stage RKN scheme and comes in the following form: $\delta x_{n,5} = \delta x_{n,3} + \dfrac{h^6}{720m^5}\{m^2 R_{61} f(x)[f'(x)]^2 + 3R_{62} m^2 f^2(x) f''(x) + 5R_{63} m p^2 f'(x) f''(x) + 6R_{64} m f(x) p^2 f^{(3)}(x) + R_{65} p^4 f^{(4)}(x)\}$, where $\delta x_{n,3}$ is set by formula (21), in which one should assume $K = 5$. The expressions for R_2, R_3, R_{41}, R_{42} in terms of polynomials P_1, P_2, P_{31}, P_{32}, P_{42}, P_{43}

Table 2. Values of RKN5-l schemes, $l = 5, 6, 7$, at $\mathrm{Det}\, V \neq 0$

Method	α_j	γ_j	$P^{(l)}_{6,\mathrm{rms}}$	κ_{cr}
5	0.2180137428269302846130 −0.6630941900724356408148 0.9162815210519267283829 0.2754877361702176563618 0.6363798707383668817883	0.6820219126111968233062 0.0016344908811675544491 0.1913562866884614688257 −0.2702137971750414591199 0.3952011069942156229473	0.7781	2.296717145585
6	0.2196475212048931979769 0.9267747775526675724223 0.2634969208444160604365 −0.3745890710865884543078 0.6405808696031580762309	0.6943833404764609973370 0.1788491925494029854970 −0.2803713165469455814716 0.0051231201077848427874 0.4020156634132967532480	0.8707	1.637899789244
7	0.1426544325995554307606 0.4972289919220082565765 0.9805992092388250425116 0.4948837279995942362020 0.6770500031205852753402	0.3426149230052762950649 0.4755156268306003353175 0.1230187470009109773628 −0.2975707328892313041635 0.3564214360524436964184	1.5344	2.760588329702

Table 3. The residuals $P_1(X)$, $P_2(X), \ldots, P_{55}(X)$ in new RKN-methods of the fifth-order accuracy

Method	P_1	P_2	P_{31}	P_{32}	P_{41}	P_{42}
5	−5.6E−17	0.0	0.0	0.0	3.1E−15	0.0
6	2.8E−17	1.1E−16	1.1E−16	2.2E−16	−1.8E−15	−2.2E−16
7	0.0	1.1E−16	−2.2E−16	2.2E−16	2.2E−16	2.8E−16
Method	P_{43}	P_{51}	P_{52}	P_{53}	P_{54}	P_{55}
5	2.2E−16	−4.4E−16	2.1E−15	1.2E−16	5.6E−17	0.0
6	0.0	0.0	3.1E−15	−3.0E−16	−3.3E−16	0.0
7	1.1E−16	2.2E−16	−2.2E−16	−1.1E−16	1.7E−16	1.1E−16

2021, **22** (2), 87–107. DOI: 10.26089/NumMet.v22r207

Table 4. The values of polynomials R_{51}, R_{52}, R_{53} at the four numerical solutions obtained in [16]

Method	R_{51}	R_{52}	R_{53}
1	−3.672E−11	−9.812E−12	3.007E−12
2	7.073E−12	1.287E−12	−5.633E−14
3	2.174E−13	6.882E−14	−1.930E−16
4	3.810E−13	1.162E−13	3.719E−16

are the same as those for the error (21), and R_{51}, R_{52},R_{53} are given by formulas (22). Further,

$$R_{61} = 1 - 720\sum_{i=1}^{K}\sum_{j=i+1}^{K}\sum_{l=j+1}^{K}(\alpha_j - \alpha_i)(\alpha_l - \alpha_j)\beta_l\gamma_i\gamma_j,$$

$$R_{62} = 1 - 120\sum_{i=1}^{K}\sum_{j=i+1}^{K}\Big[(\alpha_j - \alpha_i)^2\beta_j\gamma_i^2 + 2\sum_{l=j+1}^{K}(\alpha_l - \alpha_i)(\alpha_l - \alpha_j)\beta_l\gamma_i\gamma_j\Big],$$

$$R_{63} = 1 - 72\sum_{i=1}^{K-1}\sum_{j=i+1}^{K}(\alpha_j - \alpha_i)(\alpha_i + 2\alpha_j)\alpha_i\beta_j\gamma_i,$$

$$R_{64} = 1 - 60\sum_{i=1}^{K}\sum_{j=i+1}^{K}(\alpha_j - \alpha_i)\alpha_j^2\beta_j\gamma_i,$$

$$R_{65} = 1 - 30\sum_{i=1}^{K}\alpha_i^4\beta_i.$$

Table 4 shows the values of the polynomials R_{51}, R_{52}, R_{53} obtained after substitution of the four numerical solutions obtained in [16]. These values are at the level of machine rounding errors, from which it follows that the equation for $x(t)$ is also approximated by the RKN5 scheme with the fifth-order accuracy. One can see that methods 2 and 4 have slightly smaller values of residuals of the form $R_{5l}(X)$, $l = 1, 2, 3$, where X is the approximate solution vector from [16].

4. Stability conditions for RKN schemes. It is known that a symplectic scheme is stable when all the roots of its characteristic equation lie on the unit circle of the complex plane. As a physical model, let us consider an oscillator with quadratic potential $V(x) = m\omega^2x^2/2$, for which the equilibrium position is at $x = 0$, $p = 0$. Substituting this expression $V(x)$ into equations (4), we obtain the linear equations of motion

$$dx/dt = p/m, \qquad dp/dt = -m\omega^2x. \tag{27}$$

Let us introduce the vectors $\vec{X}^n = (x^n, p^n)^T$ and $\vec{X}^{n+1} = (x^{n+1}, p^{n+1})^T$ into consideration. In the matrix notation, equations (5) applied to system (27) have the form: $\vec{X}^{n+1} = G\vec{X}^n$, where G is a matrix of size 2×2. Let g_{ij}, $i, j = 1, 2$ be the elements of this matrix. The characteristic equation of matrix G is: $|G - \lambda E| = \lambda^2 + \mathrm{Tr}(G)\lambda + 1 = 0$, where $\mathrm{Tr}(G)$ is the trace of matrix G, $\mathrm{Tr}(G) = -g_{11} - g_{22}$; E is the identity matrix of size 2×2. The value $\mathrm{Tr}(G)$ is a function of the parameters α_j, γ_j, $j = 1, \ldots, K$, and the Courant number $\kappa = \omega h$. The stability condition of scheme (5) is the condition $|\lambda_i| \leqslant 1$, where λ_i, $i = 1, 2$ are the eigenvalues of matrix G, i.e., the roots of the characteristic equation. If the discriminant of this equation $D = [\mathrm{Tr}(G)/2]^2 - 1$ is negative, then by Vieta's theorem, it has two complex-conjugate roots λ_1, λ_2, so that $|\lambda_1| = |\lambda_2| = 1$. In this case there exists a nonzero stability region $|\kappa| \leqslant \kappa_{\mathrm{cr}}$, where κ_{cr} is the critical Courant number. Let us introduce the notation $D_2(\kappa) = |\mathrm{Tr}(G)| - 2$. For the RKN schemes considered, κ_{cr} is a solution to the equation $D_2(\kappa) = 0$, and the sought stability condition is derived from the inequality $D_2 < 0$ that follows from the inequality $D < 0$.

The symplectic schemes are known to preserve the phase volume $|G| = 1$. This relationship was used to check if the formulas for calculating the ratios of the characteristic equation are correct. The determinant $|G|$ was calculated analytically for all schemes using *Mathematica's* Simplify[Expand[Det[G]] commands, and the equality $|G| = 1$ was obtained in all cases.

2021, **22** (2), 87–107. DOI: 10.26089/NumMet.v22r207

4.1. One-stage RKN scheme. The Verlet scheme (5), $K = 1$, takes the following form when applied to linear equations (27):

$$x^{(1)} = x^n + \frac{h}{2}\frac{p^n}{m}, \qquad x^{n+1} = x^n + h\frac{p^n}{m} - \frac{h^2\omega^2}{2}x^{(1)}, \qquad p^{n+1} = p^n - hm\omega^2 x^{(1)}. \tag{28}$$

The characteristic equation $|G - \lambda E| = 0$ has the form $1 - 2\lambda + \kappa^2\lambda + \lambda^2 = 0$. This produces the formula for the discriminant $D = \kappa^2(\kappa^2/4 - 1)$. The stability condition is satisfied if $D \leqslant 0$. In the realm of positive κ numbers, this leads to the stability condition of the form $0 < \kappa \leqslant 2$ (Fig. 1).

As is known, the Hamilton equations are invertible in time with simultaneous inversion of time and particle velocities **??**. It follows that the difference symplectic schemes are also invertible in time, as are the Hamilton equations. As follows from Fig. **??**, $D \leqslant 0$ is also in the interval $[-2, 0]$ that is the Verlet scheme is stable in this interval as well. Therefore, the stability condition of this scheme should be written as $0 < |\kappa| \leqslant 2$.

4.2. Two-stage RKN scheme. The characteristic equation is not given here due to its bulkiness. In the corresponding discriminant D, we express the parameters γ_1, γ_2 through α_1, α_2 using the formulas (11). The resulting discriminant comes in the form $D = \varphi(\kappa, \alpha_1, \alpha_2)[8(\alpha_1 - \alpha_2)]^{-2} - 1$, where $\varphi(\kappa, \alpha_1, \alpha_2) = (2\alpha_2^2\kappa^4 + 2\alpha_1^2(2\alpha_2 - 1)\kappa^4 + \alpha_2(-3\kappa^4 + 4\kappa^2 - 8) - \alpha_1(4\alpha_2^2\kappa^4 - 4\alpha_2\kappa^4 + \kappa^4 + 4\kappa^2 - 8) + \kappa^4)^2$. When $l = 6$ in (14), the following expression is obtained for discriminant D: $D = 0.00082628\left(\kappa^4 - 17.3943\kappa^2 + 34.7886\right)^2 - 1$. Let us denote the roots of the equation $D = 0$ via the roots $\kappa_1, \ldots, \kappa_8$. They have the following form: $\kappa_1 = -\kappa_8$, $\kappa_2 = -\kappa_7$, $\kappa_3 = -\kappa_6$, $\kappa_4 = \kappa_5 = 0$, $\kappa_6 = 2.496957971257$, $\kappa_7 = 3.340580819059$, $\kappa_8 = 4.170644952389$. From Fig. 1 (dashed line), considering the intervals where $D \leqslant 0$, we arrive at the following stability conditions for the two-stage RKN scheme: $0 < |\kappa| \leqslant \kappa_6$, $\kappa_7 \leqslant |\kappa| \leqslant \kappa_8$.

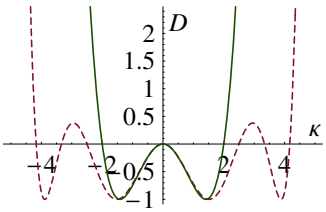

Figure 1. Discriminants $D = D(\kappa)$ for the case of the Verlet scheme (solid line) and the optimal two-stage scheme (dashed line)

4.3. A three-stage RKN scheme. The symbolic calculation of the transition matrix elements G corresponding to the three-stage scheme is performed using a *Mathematica* program developed similarly to the case of the two-stage scheme. We must note that irrespective of the number of stages in the RKN method, the transition matrix G is always of size 2×2. To simplify the expressions for the elements g_{ij}, $i, j = 1, 2$ of matrix G, the relations $P_1 = 0$, $P_2 = 0$, $P_{32} = 0$ were used.

Given the constraints $P_1 = 0$, $P_2 = 0$, $P_{32} = 0$, the trace $\mathrm{Tr}(G) = -(g_{11} + g_{22}) = -2 + \kappa^2 - \kappa^4/12 + Z\kappa^6$, where $Z = \gamma_1\gamma_2\gamma_3(\alpha_3 - \alpha_2)(\alpha_2 - \alpha_1)(1 - \alpha_3 + \alpha_1)$; besides, $|G| = 1$.

Let us find the stability region of the RKN34A scheme. The scheme is defined by parameters (17) with upper signs. Figure 2a charts the function $D_2(\kappa) = |\mathrm{Tr}(G(\kappa))| - 2$ where $\mathrm{Tr}(G) > 0$. In this case, equation $D_2(\kappa) = 0$ has two real roots $\kappa = \pm\kappa_{\mathrm{cr}}$, where $\kappa_{\mathrm{cr}} = 2\sqrt{2 + 2^{1/3} - 2^{2/3}} \approx 2.5865189$. From Fig. 2a , we can see that in the intervals $[-\kappa_{\mathrm{cr}}, 0]$ and $[0, \kappa_{\mathrm{cr}}]$ there are no intervals where $D_2(\kappa) > 0$, so the stability region of the RKN34A scheme has the form $0 < |\kappa| \leqslant \kappa_{\mathrm{cr}}$. Similar calculations for the RKN34B scheme give the same stability condition.

The RKN34C scheme is defined by parameters (18). In this case, the equation for determining κ_{cr} looks as follows: $(1/144)\kappa^2\left(\left(6 + 5\sqrt[3]{2} + 4 \cdot 2^{2/3}\right)\kappa^4 + 12\kappa^2 - 144\right) = 0$. This equation has four real roots and two complex conjugate roots. The real roots are $\kappa = 0$ (root of multiplicity 2) and $\kappa = \pm\kappa_{\mathrm{cr}}$, where $\kappa_{\mathrm{cr}} = \sqrt{6(2 - 2^{2/3})} \approx 1.573401947435$. As can be seen from Fig. 2a, the intervals $[-\kappa_{\mathrm{cr}}, 0]$ and $[0, \kappa_{\mathrm{cr}}]$ do not

Figure 2. Charts of the values $D_2 = D_2(\kappa)$: a) for RKN34A and RKN34C schemes; b) for RKN4-1a, RKN4-2a, RKN4-3a, RKN4-4a schemes

2021, **22** (2), 87–107. DOI: 10.26089/NumMet.v22r207

contain an area where $|\mathrm{Tr}(G)| - 2 > 0$; therefore, the stability region of the RKN34C scheme has the form $0 < |\kappa| \leqslant \kappa_{\mathrm{cr}}$. The RKN34A scheme has a larger stability margin than the RKN34C scheme, so the RKN34A scheme is preferable for molecular dynamics applications.

4.4. A four-stage RKN scheme. The formulas for the matrix elements G are not given here due to their bulkiness; instead we proceed straight to an expression for the trace of matrix G: $\mathrm{Tr}(G) = -2 + \kappa^2 - \kappa^4/12 + Z_6\kappa^6 + Z_8\kappa^8$, where

$$Z_6 = (\alpha_1 - \alpha_3)(1 + \alpha_1 - \alpha_4)(\alpha_3 - \alpha_4)(\gamma_1 + \gamma_2)\gamma_3\gamma_4 +$$
$$+ (\alpha_1 - \alpha_2)\gamma_2\{\alpha_4(-1 - \alpha_1 + \alpha_4)(\gamma_1 - \gamma_3)\gamma_4 - (1 + \alpha_1)\alpha_3\gamma_3(\gamma_1 + \gamma_4) + \alpha_3^2\gamma_3(\gamma_1 + \gamma_4) +$$
$$+ \alpha_2[(\alpha_4 - \alpha_3)\gamma_3\gamma_4 + \gamma_1(\gamma_3 + \alpha_1\gamma_3 - \alpha_3\gamma_3 + \gamma_4 + \alpha_1\gamma_4 - \alpha_4\gamma_4)]\},$$
$$Z_8 = (\alpha_1 - \alpha_2)(\alpha_2 - \alpha_3)(1 + \alpha_1 - \alpha_4)(\alpha_3 - \alpha_4)\gamma_1\gamma_2\gamma_3\gamma_4.$$

In the general case where $\mathrm{Det}\, V \neq 0$ (Table 1), RKN4 schemes have been found that have a much smaller leading error term than the schemes obtained in the special cases of the Vandermonde determinant turning to zero. We found the κ_{cr} values for all the schemes listed in Table 1. The respective charts of $D_2 = D_2(\kappa) = Tr(G(\kappa)) - 2$ are presented in Fig. 2b. It follows from this figure that the stability region for all the four schemes is described by the inequalities $0 < |\kappa| \leqslant \kappa_{\mathrm{cr}}$. The leading error term in each of the four schemes in Table 1 is almost three times smaller than in the case of the schemes obtained in the special cases of the Vandermonde determinant turning to zero. Therefore, the schemes presented in Table 1 are preferable when solving applied problems.

4.5. A five-stage RKN scheme. In the case in question, the trace $Tr(G) = -2 + \kappa^2 - \kappa^4/12 + 0.002777777778\kappa^6 + Z_8\kappa^8 + Z_{10}\kappa^{10}$. The expressions for Z_8, Z_{10} are not given here due to their bulkiness. In [16], the authors present tables of α_j, γ_j $(j = 1, \ldots, 5)$ parameter values for four methods, which we call RKN5-1, RKN5-2, RKN5-3, RKN5-4. Below is the form of equations $D_2(\kappa) = 0$ and the corresponding stability conditions we obtained for each of the four methods. The behavior of curves $D_2(\kappa) = |\mathrm{Tr}(G(\kappa))| - 2$ at $\mathrm{Tr}(G) > 0$ (Fig. 3) was taken into consideration.

RKN5-1, RKN5-3, $Tr(G) > 0$:

$$-4 + \kappa^2 - \kappa^4/12 + 0.002777777778\kappa^6 + 0.019206667644\kappa^8 + 0.001488249575\kappa^{10} = 0,$$

stability region: $0 < |\kappa| \leqslant 1.709678742327$.

RKN5-2, RKN5-4, $Tr(G) > 0$:

$$-4 + \kappa^2 - \kappa^4/12 + 0.002777777778\kappa^6 + 0.009374405183\kappa^8 + 0.000595080910\kappa^{10} = 0,$$

stability region: $0 < |\kappa| \leqslant 1.836026193724$.

At $\mathrm{Tr}(G) < 0$, the roots of the equation $-\mathrm{Tr}(G) - 2 = 0$ are grouped similarly for all four methods: there is a root $\kappa = 0$ of multiplicity 2, four purely imaginary roots, and two pairs of complex conjugate roots.

After conducting the analysis, we conclude that RKN5-2 and RKN5-4 methods have a slightly larger stability region than the RKN5-1 and RKN5-3 methods. Furthermore, as shown in 3.5, the weighted RMS value of the polynomials $1, P_{61}, \ldots, P_{66}$ in the case of RKN5-2 and RKN5-4 methods is smaller than in the

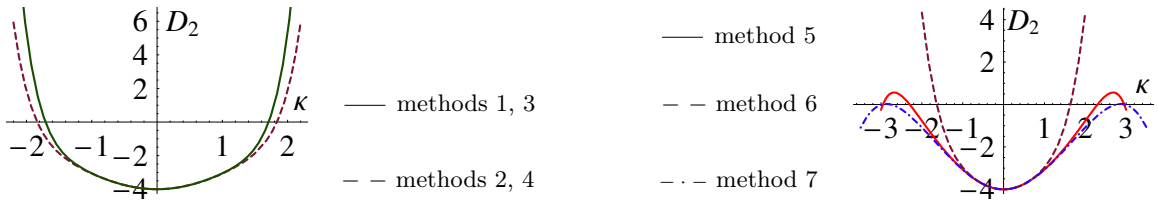

a) b)

Figure 3. Charts of the curves $D = D(\kappa)$ for RKN5 schemes considered in [16]:
a) For methods 1 to 4; b) For methods 5 to 7

2021, **22** (2), 87–107. DOI: 10.26089/NumMet.v22r207

case of RKN5-1 and RKN5-3 methods. Therefore, RKN5-2 and RKN5-4 are the preferred methods for use in molecular dynamics problems, compared to RKN5-1 and RKN5-3.

For methods 5, 6, 7 (Table 2) the equations $D_2(\kappa) = |\mathrm{Tr}(G(\kappa))| - 2 = 0$ have the following form at $\mathrm{Tr}(G) > 0$:

Method 5:

$$-4 + \kappa^2 - \kappa^4/12 + 0.014070112667\kappa^6 - 0.001296648123\kappa^8 + 4.263921514569 \cdot 10^{-6}\kappa^{10} = 0,$$

stability region: $0 < |\kappa| \leqslant 2.296717145585$.

Method 6:

$$-4 + \kappa^2 - \kappa^4/12 + 0.120356465194\kappa^6 - 0.007649609920\kappa^8 + 0.000075698663\kappa^{10} = 0,$$

stability region: $0 < |\kappa| \leqslant 1.637899789244$.

Method 7:

$$-4 + \kappa^2 - \kappa^4/12 + 0.005858440103\kappa^6 - 0.000521738767\kappa^8 + 0.000015008970\kappa^{10} = 0,$$

stability region: $0 < |\kappa| \leqslant 2.760588329702$.

According to Table 2, method 5 is the best in terms of the smallness of the leading error term; in addition, the value of κ_{cr} in this method is 1.25 times larger than in the case of methods 2 and 4 of [16].

4.6. Comparison of the efficiency of the considered RKN schemes. The main computational effort of RKN schemes is related to computing the function $f(x)$ included in (4). To calculate the values of x^{n+1}, p^{n+1} using the K-stage RKN scheme, we must calculate values K of the function $f(x)$. At first sight, the machine time required should increase linearly with the number of stages. But we should also take into account the value of the critical Courant number κ_{cr}, which is different for different RKN schemes. In the case of applying ordinary (non-symplectic) Runge-Kutta schemes for numerical solution of aerodynamics problems in [18, 19] it was shown that as the number of stages of the explicit Runge-Kutta scheme increases, the value of the Courant critical number also increases. Therefore it is possible to carry out stable calculations with larger values of the Courant number than in the case of Runge-Kutta schemes with a small number of stages. This can ultimately lead to a reduction in the machine time required to solve the problem. In this regard, a quantitative characterization of the efficiency of Runge-Kutta schemes was first introduced in [18], which will be denoted by *ef*: $ef = \kappa_{\mathrm{cr}}/K$. [18, 19] provided values of the efficiency parameter *ef* for a number of explicit Runge-Kutta schemes, which are still widely used in aerodynamic calculations.

The value of *ef* can also be calculated for each of the RKN schemes discussed above. Results of these calculations are presented in Table 5. In particular, the *ef* value in RKN34A scheme is 1.56 times higher than in the RKN34C scheme.

Table 5 shows that as the number of stages K increases, the value of *ef* decreases. This is the essential difference between explicit symplectic RKN schemes and explicit non-symplectic Runge-Kutta schemes.

Table 5. Efficiency index *ef* for a number of RKN schemes

RKN scheme	K	κ_{cr}	*ef*
Verlet	1	2	2
$\alpha_1 = 0.17922$, $\alpha_2 = 0.82078$	2	4.17064	2.08532
RKN34A scheme	3	2.58652	0.86217
RKN34C scheme	3	1.57340	0.52447
RKN4-1a scheme	4	2.60111	0.65028
RKN5 scheme, methods 1, 3	5	1.70968	0.34193
RKN5 scheme, methods 2, 4	5	1.83603	0.36721
RKN5 scheme, method 5	5	2.29672	0.45934

5. The Kepler problem. The problem on the motion of a system consisting of two interacting particles (two-body problem, Kepler problem) allows for a complete analytical solution in general terms [3]. The potential energy U of the interaction of two particles depends only on the distance between them, i.e., on the absolute value of the difference of their radius vectors. Let's consider a special case when both particles move in the plane (x, y). The Hamiltonian of such system has the following form:

$$H = |\boldsymbol{p}_1|^2/(2m_1) + |\boldsymbol{p}_2|^2/(2m_2) + U(|\boldsymbol{r}_1 - \boldsymbol{r}_2|),$$

where $\vec{p}_1, \vec{p}_2$ are the vectors of the momentums of the first and second particle, $\vec{p}_j = (m_j u_j, m_j v_j)$, $\vec{r}_j = (x_j, y_j)$, $j = 1, 2$, m_j is the mass of the jth particle, u_j and v_j are the components of the velocity vector of the jth particle along the axes x and y, respectively; $|\vec{p}_j|^2/(2m_j) = m_j(u_j^2 + v_j^2)/2$ is the kinetic energy of the jth

2021, **22** (2), 87–107. DOI: 10.26089/NumMet.v22r207

particle. The potential energy is specified in the form

$$U(|\boldsymbol{r}_1 - \boldsymbol{r}_2|) = -\tilde{G}m_1m_2/|\boldsymbol{r}_1 - \boldsymbol{r}_2|,$$

where $\tilde{G}$ is the gravitational constant.

Below we consider the special case when $m_1 = m_2 = 1$, $\tilde{G} = 1$. Let us introduce the notation $\boldsymbol{p}_j = (p_{jx}, p_{jy})$, $j = 1, 2$. Then the solution of the problem in question is reduced to solving the following system of ordinary differential equations:

$$\begin{aligned} &\frac{dp_{1x}}{dt} = -\frac{(x_1 - x_2)}{r^3}, \quad &&\frac{dx_1}{dt} = p_{1x}, \quad &&\frac{dp_{1y}}{dt} = -\frac{(y_1 - y_2)}{r^3}, \quad &&\frac{dy_1}{dt} = p_{1y}, \\ &\frac{dp_{2x}}{dt} = \frac{(x_1 - x_2)}{r^3}, \quad &&\frac{dx_2}{dt} = p_{2x}, \quad &&\frac{dp_{2y}}{dt} = \frac{(y_1 - y_2)}{r^3}, \quad &&\frac{dy_2}{dt} = p_{2y}. \end{aligned} \tag{29}$$

Here r is the distance between two particles, $r = |\boldsymbol{r}_1 - \boldsymbol{r}_2| = \sqrt{(x_1 - x_2)^2 + (y_1 - y_2)^2}$, and we assume that x_1, y_1, x_2, y_2, p_{1x}, p_{1y}, p_{2x}, p_{2y} are time-dependent functions t.

The system (29) is solved under the following initial conditions given at $t = 0$ (Fig. 4a):

$$\begin{aligned} &x_1(0) = a_0, \quad &&y_1(0) = 0, \quad &&x_2(0) = -a_0, \quad &&y_2(0) = 0, \\ &p_{1x}(0) = 0, \quad &&p_{1y}(0) = v_0, \quad &&p_{2x}(0) = 0, \quad &&p_{2y}(0) = -v_0, \end{aligned} \tag{30}$$

where a_0 is a set positive number, v_0 is the absolute initial velocity value of each particle in the direction of the y axis; the value $v_0 > 0$ is a set value.

According to the Noether's theorem [3], at $t > 0$ the total energy E should remain constant for a system of two particles. Taking into account (30) we obtain:

$$|E| = |H| = |v_0^2 - 1/(2a_0)|. \tag{31}$$

As shown in [3], the motion of a two-body system is finite at $E < 0$, and infinite at $E > 0$. The case of finite motion is considered below. To ensure finiteness, the constants v_0 and a_0 must satisfy the inequality $v_0^2 - 1/(2a_0) < 0$. In this case, the motion of each particle at $t > 0$ occurs along its own elliptical orbit. Let us introduce the mutual distance vector of the two points $\boldsymbol{r} = \boldsymbol{r}_2 - \boldsymbol{r}_1$ and place the origin of coordinates at the center of inertia, which produces the equality $m_1\boldsymbol{r}_1 + m_2\boldsymbol{r}_2 = 0$. Proceeding from the last two equalities, we find:

$$\boldsymbol{r}_1 = -\frac{m_2}{m_1 + m_2}\,\boldsymbol{r}, \qquad \boldsymbol{r}_2 = \frac{m_1}{m_1 + m_2}\,\boldsymbol{r}. \tag{32}$$

The value $m = m_1m_2/(m_1 + m_2)$ is called reduced mass; since in our case $m_1 = m_2 = 1$, then $m = 1/2$. In order to obtain the complete solution of the two-body problem, we need to find the formula for $\boldsymbol{r} = (x(t), y(t))$ in accordance with (32). The formula is given in [3]:

$$x = a(\cos\xi - e), \qquad y = a\sqrt{1 - e^2}\,\sin\xi. \tag{33}$$

Here a is the major semiaxis of the ellipse, e is the eccentricity of the elliptical orbit,

$$a = \alpha/(2|E|), \qquad e = \sqrt{1 + 2EM^2/(m\alpha^2)}. \tag{34}$$

a) *b)*

Figure 4. Particle trajectories: a) Initial velocity vectors for the system (29); b) the result of numerical solution by all RKN methods at $e = 0$

2021, **22** (2), 87–107. DOI: 10.26089/NumMet.v22r207

Here $\alpha = \tilde{G}m_1m_2 = 1$ according to the values of $\tilde{G}$, m_1, m_2 chosen above; M is the value of the momentum vector directed along the normal to the plane (x, y). The law of conservation of momentum [3] states: $M = \text{const}$ $\forall t \geqslant 0$. From the initial conditions (30) we obtain: $M = 2a_0v_0$, where $2a_0$ is the initial distance between the particles.

From (32) and (33) it follows that at $e = 0$ the particles move in circles. This fact can be used for additional verification of the computer program implementing the RKN method for solving the two-body problem. Let us find the condition for the parameters a_0, v_0 at which $e = 0$. By substituting the expressions for E, M and α in (34), we arrive at

$$e^2 = 1 + 2EM^2/(m\alpha^2) = 1 + 4(v_0^2 - 1/(2a_0))4a_0^2v_0^2 = (4a_0v_0^2 - 1)^2 = 0. \tag{35}$$

It follows that to ensure zero eccentricity it is sufficient to assume $v_0 = 0.5/\sqrt{a_0}$. In particular, at $a_0 = 2$ we have: $v_0 = 0.5/\sqrt{2} \approx 0.35355$. Further, the eccentricity $e > 0$ is satisfied if the following inequalities are satisfied: either $4a_0v_0^2 < 1$, or $\frac{1}{4} < a_0v_0^2 < \frac{1}{2}$. The inequality $a_0v_0^2 < \frac{1}{2}$ provides the finiteness of motion of both particles taking into account (31).

In the case of the two-body problem, we have the following vector-column of required quantities: $\boldsymbol{X} = (x_1, p_{1x}, y_1, p_{1y}, x_2, p_{2x}, y_2, p_{2y})^T$, where T is an index denoting the transpose operation. In order to apply the K-stage RKN method to solve the problem in question, we must replace the vector-column $(x, p)^T$ by $\boldsymbol{X}$ in (5). As a result, a system of eight ordinary differential equations (29) needs to be solved.

In order to verify the developed FORTRAN program, we carried out calculations of the two-body problem by all RKN schemes with the number of stages $K = 1, 2, 3, 4, 5$ for the cases of zero and non-zero eccentricity e in (34), as discussed in the previous sections. The numerical solution for the coordinates of both particles, obtained at $e = 0$ by all considered RKN methods after performing 7140 time steps with constant step $h = 0.005$, is shown in Fig. 4b. The coordinates of the particles were memorized every 80 steps by t. It is seen that both particles move along the same circular orbit. Using the formula (15.8) from [3], it is easy to find the time period T needed for a particle to make a complete revolution in a circular orbit in case of zero eccentricity: $T = \pi\sqrt{a}$, where a is the radius of the circle along which each particle moves; in our case $a = 2$. From here, it is easy to find that for time $t = 35.7$ each of two particles has made 8 complete revolutions in a circle.

Table 6 presents the calculation results of the problem two particles moving along the circular orbit by all five RKN schemes considered in the previous sections. The values δE_{mean} and $|\delta E|_{\text{mean}}$ were calculated as the arithmetic mean of the values δE^n and $|\delta E^n|$, where $\delta E^n = (E^n - E_0)/E_0$, $E^n = (1/2)[(p_{1x}^n)^2 + (p_{1y}^n)^2 + (p_{2x}^n)^2 + (p_{2y}^n)^2] - 1/r^n$, $E_0 = v_0^2 - 1/(2a_0)$ in accordance with (31), $r^n = [(x_1^n - x_2^n)^2 + (y_1^n - y_2^n)^2]^{1/2}$. Moreover, $\delta r_{m,\max}$ is the maximum relative deviation of the magnitude of the radius-vector r^n of the mth particle $(m = 1, 2)$ from the exact radius $a = 2$ of the circular orbit, i.e. $\delta r_{m,\max} = \max\limits_j \left(\sqrt{x_{mj}^2 + y_{mj}^2} - a\right)/a$. It turned out that at least the first 14 digits of the decimal mantissa are the same for the numbers $\delta r_{1,\max}$ and $\delta r_{2,\max}$. Therefore, only the value $\delta r_{1,\max}$ is given in Table 6. From the point of view of practical applications, the most important is

Table 6. Errors δE_{mean}, $|\delta E|_{\text{mean}}$ and $\delta r_{m,\max}$ at $e = 0$ for different RKN methods

K	RKN scheme	Error of the scheme	δE_{mean}	$\lvert\delta E\rvert_{\text{mean}}$	$\delta r_{1,\max}$
1	(Verlet)	$O(h^2)$	−1.783E−14	1.783E−14	1.953E−7
2	$\alpha_1 = \alpha_1^{(6)}, \alpha_2 = \alpha_2^{(6)}$	$O(h^2)$	−7.879E−15	7.889E−15	9.605E−8
3	RKN34A	$O(h^4)$	−3.918E−15	4.048E−15	5.684E−14
4	RKN4-1a	$O(h^4)$	1.703E−15	3.663E−15	6.706E−14
5	RKN5-2	$O(h^5)$	−5.876E−15	5.957E−15	1.510E−14

Table 7. Errors δE_{mean}, $|\delta E|_{\text{mean}}$ and $\delta r_{m,\max}$ at $e = 0$ for the fourth-order accuracy methods from Table 1

RKN scheme	δE_{mean}	$\lvert\delta E\rvert_{\text{mean}}$	$\delta r_{1,\max}$
RKN4-1a	1.703E−15	3.663E−15	6.706E−14
RKN4-2a	−3.378E−15	3.462E−15	2.243E−14
RKN4-3a	−4.781E−15	5.126E−15	3.331E−14
RKN4-4a	−2.504E−15	2.609E−15	1.954E−14

2021, **22** (2), 87–107. DOI: 10.26089/NumMet.v22r207

Table 8. Errors δE_{mean}, $|\delta E|_{\text{mean}}$ and $\delta r_{m,\max}$ at $e = 0$ for the fifth-order accuracy methods from Table 3

RKN scheme	δE_{mean}	$\lvert\delta E\rvert_{\text{mean}}$	$\delta r_{1,\max}$
RKN5-5	−4.270E−15	4.407E−15	6.128E−14
RKN5-6	−5.679E−15	5.785E−15	5.973E−14
RKN5-7	2.598E−15	2.710E−15	2.087E−14

Table 9. Errors δE_{mean}, $|\delta E|_{\text{mean}}$ and $\delta y_{1,\,\text{mean}}$ at $v_0 = 0.2$ for different RKN methods

K	δE_{mean}	$\lvert\delta E\rvert_{\text{mean}}$	$\delta y_{1,\,\text{mean}}$
1	2.749E−7	2.749E−7	−3.384E−5
2	8.754E−8	8.838E−8	−1.067E−5
3	5.438E−13	6.230E−13	−2.762E−7
4	6.047E−13	5.753E−13	−2.762E−7
5	−5.512E−15	9.388E−15	−2.761E−7

the accuracy of calculating the point coordinates $(x_m^n,\, y_m^n)$. Table 6 shows that the best accuracy in calculating these coordinates is achieved using the five-step RKN scheme.

From the comparison of Tables 6 and 7, it can be seen that the new RKN4-4a scheme provides lower errors in δE_{mean} energy values, $|\delta E|_{\text{mean}}$, than the RKN4-2 method. Further, a comparison of Tables 6 and 8 shows that the new RKN schemes of fifth-order accuracy provide lower errors in δE_{mean} energy values, $|\delta E|_{\text{mean}}$, than method 2 from [16].

In order to consider the case of each particle moving along its own elliptical orbit, let us assume $v_0 = 0.2$, $a_0 = 2$ in (30). This satisfies the inequality $4a_0v_0^2 < 1$, so the eccentricity $e \neq 0$ and $E < 0$. Each particle makes one complete revolution in an elliptical orbit in time [3] $T = \pi\alpha\sqrt{m/(2|E|^3)}$. By substituting the values $\alpha = 1$, $m = 1/2$, $E = v_0^2 - 1/(2a_0)$, we arrive at $T = 16.3227$. If we set physical time $t = 164$, then each particle will make 10 complete revolutions in its elliptical orbit. The numerical solution for the coordinates of both particles, obtained by all considered RKN methods at $t = 164$ after performing 82,000 time steps with the step $h = 0.002$, is shown in Fig. 5. The coordinates of the particles were memorized every 100 steps by t. We can see that each particle moves along its elliptical orbit, and positions of the particles agree very well with exact elliptical orbits.

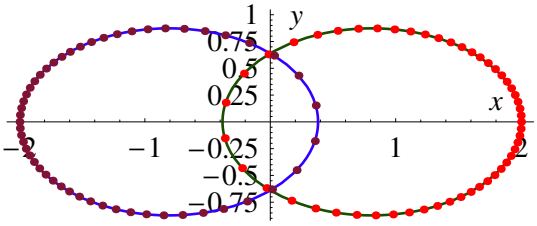

Figure 5. Elliptical orbits of particle 1 (right ellipse) and particle 2 (left ellipse) in the interval $0 < t \leqslant 164$. Solid lines are exact ellipses, dotted lines are a numerical solution obtained by RKN method

Table 9 presents the values of relative errors δE_{mean} and $|\delta E|_{\text{mean}}$ obtained in the numerical solution of the two-body problem for two particles moving along elliptical orbits by all five RKN schemes considered in the previous sections. Note that in the case of the RKN scheme of the fifth-order accuracy, these errors are two decimal orders smaller than in the case of the fourth-order accuracy scheme (Fig. 6).

The value of $\delta y_{1,\,\text{mean}}$ was calculated as the arithmetic mean of the values $\delta y_{1j} = y_{1j} - y_{1,\,\text{ex}}$. Here $y_{1,\,\text{ex}}$ is the exact value of the coordinate y at the intersection of the line $x = x_{1j}$ with the ellipse of the first particle (see the right ellipse in Fig. 5). At a fixed value of x from the exact equation for the coordinate $x = -0.5a(\cos\xi - e)$ for the first particle in elliptical orbit, we derive the argument $\xi_j = \arccos[e - (2x_{1j}/a)]$. After that the exact value of the coordinate y of the point lying on the ellipse is found by the formula: $y_{1,ex} = 0.5b \cdot \text{sign}(y_{1j}) \sin\xi_j$. The value $\delta y_{2,\,\text{mean}}$ is calculated in a similar way, by using exact formulas for the ellipse of the second particle. It turned out that the first ten digits of mantissa of machine numbers $\delta y_{1,\,\text{mean}}$ and $\delta y_{2,\,\text{mean}}$ are the same, but the signs of these numbers are opposite. For example, at $K = 5$, the value $\delta y_{2,\,\text{mean}} = +2.761e-7$ was obtained.

In general, the error δy_{1j} is much larger than δE_{mean}. A detailed examination of the local errors δy_{1j} in the case of the five-stage scheme for each value of $x = x_{1j}$ has shown that the error increases in absolute

2021, **22** (2), 87–107. DOI: 10.26089/NumMet.v22r207

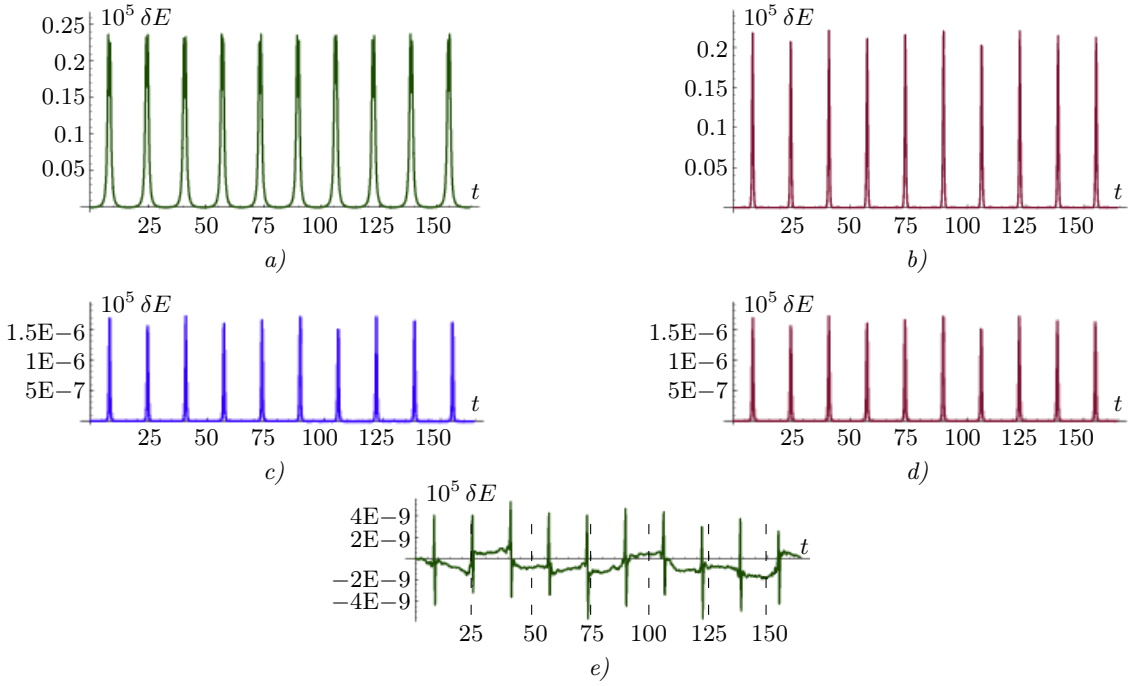

Figure 6. The Kepler problem, the case of nonzero eccentricity. Values $10^5\delta E$ as a function of time at different number of stages K in RKN methods: *a)* $K = 1$, *b)* $K = 2$, *c)* $K = 3$, *d)* $K = 4$, *e)* $K = 5$

magnitude to a value of about 10^{-5} near the x axis at $|y_{1j}| < 0.1$, that is where the ellipse curvature is greatest. In the case when the particles move along a circular orbit (at $e = 0$), the problem does not arise, since the curvature of the circle is constant (see Table 6).

As can be easily seen in Fig. 6, at each K the number of bursts equals 10, i.e., the number of periods of each particle's motion in its elliptical orbit. To explain this phenomenon, let us turn to Fig. 7. In this figure $r = r(t) = |\boldsymbol{r}_1 - \boldsymbol{r}_2|$. The shape of the curve shown in this figure is the same for all RKN schemes considered. We see that the curve $r(t)$ has 10 minima. At each minimum, the curvature radius is very small. The curvature is inversely proportional to the curvature radius, so it is clear that it reaches the maximum at the minima of function $r(t)$. In turn, the curvature is proportional to the second derivative of this function. Therefore, this derivative has the largest absolute value at the minima of the function $r(t)$. The second- and higher-order derivatives of functions $x(t), y(t)$ are included in the leading error terms in the RKN methods. It follows that the scheme error should increase at the minima of the function $r(t)$, which is observed in Fig. 6.

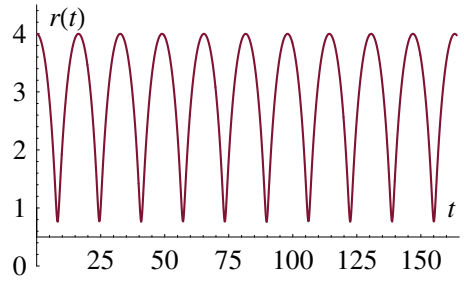

Figure 7. Chart of the curve $r(t) = |\boldsymbol{r}_1 - \boldsymbol{r}_2|$ at non-zero eccentricity e

It follows from (35) that the eccentricity $e = |4a_0v_0^2 - 1|$ increases with decreasing v_0. Table 10 shows the relative errors δE_{mean} and $|\delta E|_{\text{mean}}$ obtained at $v_0 = 0.15$, $h = 0.005$. The calculations were performed up to time $T = 500$; 10^5 time steps were taken. During this time, each of the two particles made more than 34 complete revolutions in an elliptical orbit. Comparing Tables 9 and 10, one can see that the relative errors of the energy conservation law have increased by two to three decimal orders of magnitude as compared to the

Table 10. Errors δE_{mean}, $|\delta E|_{\text{mean}}$ and $\delta y_{1,\,\text{mean}}$ at $v_0 = 0.15$ for different RKN methods

K	δE_{mean}	$\lvert\delta E\rvert_{\text{mean}}$	$\delta y_{1,\,\text{mean}}$
1	8.361E−6	8.361E−6	−5.053E−3
2	2.954E−6	3.174E−6	−1.581E−3
3	9.686E−10	9.686E−10	−1.630E−7
4	9.686E−10	9.686E−10	−1.630E−7
5	4.157E−12	2.292E−11	+1.023E−6

2021, **22** (2), 87–107. DOI: 10.26089/NumMet.v22r207

case of $v_0 = 0.2$. The following reasons for the decrease in accuracy can be pointed out: first, the calculations were performed up to a time moment $T = 500$, which is three times larger than the time moment $T = 164$. Second, the step $h = 0.005$ was used, which is 2.5 times the step with which the calculations for Table 9 were made. Third, at $v_0 = 0.15$, the minor semiaxes of the ellipses are smaller than at $v_0 = 0.2$. This led to an increase in the curvature of ellipses in the vicinity of the x-axis. As in the case of Table 9, the RKN scheme of the fifth-order accuracy is the most accurate one, compared to the schemes of lower orders of accuracy.

6. Conclusion. Explicit symplectic Runge-Kutta-Nyström (RKN) difference schemes with 1 to 5 stages have been reviewed for numerical solution of molecular dynamics problems described by systems with separable Hamiltonians. For 2- and 3-stage RKN schemes, the parameters are obtained using the Gröbner basis technique. For 4 and 5 stages, new schemes are found using Nelder-Mead numerical optimization method. In particular, four new schemes were obtained for stages numbering 4. In addition to the four schemes known in the literature, three new schemes were obtained for stages numbering 5. For each specific number of stages, the best scheme in terms of the minimum leading term of the approximation error is found. Stability conditions for all the schemes in question were obtained, including new schemes.

A generalization of the notion of efficiency ef for a multistage non-symplectic Runge-Kutta scheme in the cases of multistage symplectic RKN schemes is proposed. It is shown that the value of ef decreases with increasing number of K stages. This is the essential difference between the symplectic RKN schemes and the explicit non-symplectic Runge-Kutta schemes, widely used nowadays in computational fluid dynamics.

By applying the RKN-methods under consideration to numerical solution of the Kepler problem with an exact solution, it was discovered that increasing the number of stages K results in higher accuracy of the particle energy conservation law. This makes RKN schemes of high orders of accuracy preferable when solving applied problems over a large time interval.

The RKN schemes considered are explicit, which makes it especially convenient to parallelize the computations for these schemes.

References

1. S. P. Kiselev, E. V. Vorozhtsov, and V. M. Fomin, *Foundations of Fluid Mechanics with Applications: Problem Solving Using Mathematica* (Birkhäuser, Boston, 1999).
2. S. K. Godunov, S. P. Kiselev, I. M. Kulikov, and V. I. Mali, *Modeling of Shockwave Processes in Elastic-plastic Materials at Different (Atomic, Meso and Thermodynamic) Structural Levels* (Inst. Komp'yut. Issled., Moscow–Izhevsk, 2014) [in Russian].
3. L. D. Landau and E. M. Lifshitz, *Course of Theoretical Physics*, Vol. 1: *Mechanics* (Nauka, Moscow, 1973; Pergamon, Oxford, 1977).
4. H. R. Lewis, D. C. Barnes, and K. J. Melendez, "The Liouville Theorem and Accurate Plasma Simulation," J. Comput. Phys. **69** (2). 267–282 (1987).
5. R. D. Ruth, "A Canonical Integration Technique," IEEE Trans. Nucl. Sci. **NS-30** (4), 2669–2671 (1983).
6. M. Tuckerman and B. J. Berne, "Reversible Multiple Time Scale Molecular Dynamics," J. Chem. Phys. **97** (3), 1990–2001 (1992).
7. E. Forest and R. D. Ruth, "Fourth-Order Symplectic Integration," Physica D **43** (1), 105–117 (1990).
8. I. P. Omelyan, I. M. Mryglod, and R. Folk, "Optimized Verlet-like Algorithms for Molecular Dynamics Simulations," Phys. Rev. E **65** (2002). doi 10.1103/PhysRevE.65.056706.
9. E. J. Nyström, *Über die numerische Integration von Differentialgleichungen* (Acta Soc. Sci. Fenn., Helsingfors, 1925) [in German].
10. L. Verlet, "Computer 'Experiments' on Classical Fluids. I. Thermodynamical Properties of Lennard–Jones Molecules," Phys. Rev. **159** (1), 98–103 (1967).
11. 11. Yu. B. Suris, "The Canonicity of Mappings Generated by Runge–Kutta Type Methods when Integrating the Systems $\ddot{x} = -\partial U/\partial x$," Zh. Vychisl. Mat. Mat. Fiz. **29** (2), 202–211 (1989) [USSR Comput. Math. Math. Phys. **29** (1), 138–144 (1989)].
12. V. N. Sofronov and V. E. Shemarulin, "Classification of Explicit Three-Stage Symplectic Difference Schemes for the Numerical Solution of Natural Hamiltonian Systems: A Comparative Study of the Accuracy of High-Order Schemes on Molecular Dynamics Problems," Zh. Vychisl. Mat. Mat. Fiz. **56** (4), 551–571 (2016) [Comput. Math. Math. Phys. **56** (4), 541–560 (2016)].
13. E. Hairer, S. P. Nørsett, and G. Wanner, *Solving Ordinary Differential Equations I: Nonstiff Problems* (Spinger, Berlin, 1993; Mir, Moscow, 1990).
14. W. W. Adams and P. Loustaunau, *An Introduction to Gröbner Bases. Graduate Studies in Mathematics. Vol. 3. (Amer. Math. Soc., Providence, 1996).*

2021, **22** (2), 87–107. DOI: 10.26089/NumMet.v22r207

15. J. A. Nelder and R. Mead, "A Simplex Method for Function Minimization," Computer J. **7** (4), 308–313 (1965).
16. D. I. Okunbor and R. D. Skeel, "Canonical Runge–Kutta–Nyström Methods of Orders Five and Six," J. Comput. Appl. Math. **51** (3), 375–382 (1994).
17. D. Okunbor and R. D. Skeel, "Explicit Canonical Methods for Hamiltonian Systems," Math. Comput. **59** (200), 439–455 (1992).
18. 18. W. Schmidt and A. Jameson, "Euler Solvers as an Analysis Tool for Aircraft Aerodynamics," in *Advances in Computational Transonics* (Pineridge Press, Swansea, 1985), pp. 371–404.
19. 19. V. G. Ganzha and E. V. Vorozhtsov, *Computer-Aided Analysis of Difference Schemes for Partial Differential Equations* (Wiley, New York, 2012).

Received
February 16, 2021

Accepted for publication
April 14, 2021

Information about the authors

Evgenii V. Vorozhtsov — Dr. Sci., Professor, Leading Scientist, Khristianovich Institute of Theoretical and Applied Mechanics, Siberian Branch of Russian Academy of Sciences, Institutskaya ulitsa 4/1, 630090, Novosibirsk, Russia.

Sergey P. Kiselev — Dr. Sci., Professor, Leading Scientist, Khristianovich Institute of Theoretical and Applied Mechanics, Siberian Branch of Russian Academy of Sciences, Institutskaya ulitsa 4/1, 630090, Novosibirsk, Russia.